Dynamic Relational Priming Improves Transformer in Multivariate Time Series

Anonymous authors
Paper under double-blind review

Abstract

Standard attention mechanisms in transformers employ static token representations that remain unchanged across all pair-wise computations in each layer. This limits their representational alignment with the potentially diverse relational dynamics of each token-pair interaction. While they excel in domains with relatively homogeneous relationships, standard attention's static relational learning struggles to capture the heterogeneous inter-channel dependencies of multivariate time series (MTS) data where different channel-pair interactions within a single system may be governed by entirely different physical laws or temporal dynamics. To better align the attention mechanism for such domain phenomena, we propose attention with dynamic relational priming (prime attention). Unlike standard attention where each token presents an identical representation across all of its pair-wise interactions, prime attention tailors each token dynamically (or per interaction) through learnable modulations to best capture the unique relational dynamics of each token pair, optimizing each pair-wise interaction for that specific relationship. This representational plasticity of prime attention enables effective extraction of relationship-specific information in MTS while maintaining the same asymptotic computational complexity as standard attention. Our results demonstrate that prime attention consistently outperforms standard attention across benchmarks, achieving up to 6.5% improvement in forecasting accuracy. In addition, we find that prime attention achieves comparable or superior performance using up to 40% less sequence length compared to standard attention, further demonstrating its superior relational modeling capabilities.

1 Introduction

An important challenge in applying transformers to multivariate time series (MTS) stems from domain mismatch. While transformers excel in domains like natural language processing (Bahdanau et al., 2014; Vaswani et al., 2017; Achiam et al., 2023; Devlin et al., 2019), computer vision (Guo et al., 2022; Carion et al., 2020; Dosovitskiy et al., 2020), and graph representation learning (Yun et al., 2019; Joshi, 2025; Veličković et al., 2017; Rampášek et al., 2022) where relationships exhibit relatively homogeneous interaction patterns amenable to uniform computational treatment, MTS data can exhibit exponentially richer heterogeneous inter-channel dependencies that resist such standardized processing. In language modeling, token relationships are predominantly semantic in nature, enabling most critical patterns to be captured by simple weighted sums of token representations. Similarly, in computer vision, spatial relationships dominate, enabling attention mechanisms to focus on regions of interest through uniform spatial reasoning. Learning on graphs exhibits comparable homogeneity, where node relationships are fundamentally structural and connectivity-based, allowing standard attention to model interactions through meaningful topological patterns (that are sometimes separated by relationship type (Schlichtkrull et al., 2018; Hu et al., 2020; Wang et al., 2019)). In these domains, representational uniformity aligns with the underlying relational homogeneity, enabling effective pattern discovery through weighted aggregation of static token representations. By static, we mean that token representations in each layer are fixed relative to all other tokens throughout pair-wise modeling. In other words, in standard attention, a given token presents the same representational perspective of itself across all of its pair-wise interactions with other tokens. We classify this property of standard attention mechanisms as **static relational learning**.

On the other hand, MTS data can exhibit qualitatively different heterogeneity within individual systems. Indeed, different token (or channel) pairs within the same system can display fundamentally distinct relational patterns. Furthermore, different channel-pairs within an MTS system may be subject to fundamentally distinct physical laws or temporal dynamics that may actually hinder the model learning process unless the underlying relationships are properly discovered. For example, temperature-pressure sensor relationship may be governed by different temporal dynamics than temperature-flow sensor relationship. This pair-wise heterogeneity suggests that the static and uniform computational treatment of tokens in standard attention may not adequately capture the distinct physical laws, causal mechanisms, and temporal dynamics that govern each unique channel-pair within MTS systems. For example, if token A experiences lead-lag with token B but has instantaneous correlations with token C, then the relational modeling process could benefit from token A's representation being modulated differently for interacting with token B than for token C to ensure representational compatibility in each interaction. Standard attention's static relational learning cannot achieve this dynamic modulation of token A and instead forces the same representational perspective of token A on both tokens B and C, potentially undermining the effective discovery of useful patterns that are unique to each pair-wise interaction.

We propose attention with dynamic relational priming (**prime attention**) to better align the attention mechanism for the requirements of the MTS domain. Dynamic priming customizes token representations for each specific pair-wise interaction, optimizing for computational alignment between tokens based on their relationship characteristics. We denote this property of prime attention as **dynamic relational learning** and formalize both static and dynamic relational learning in Section 4. When token A interacts with token B, learnable modulation primes A's representation to align computationally with the A-B relationship dynamics; when the same token A interacts with token C, a different primer transforms A's representation to better align with the distinct A-C relationship requirements. This pair-specific priming process enables each interaction to access representational views specifically optimized for their unique relational patterns, transcending the one-size-fits-all constraints of standard attention and static relational learning. For example, the primer for token A-B relationship may amplify parts of token A's representation that offer the most relevant lead-lag information with respect to token B. For token A-C relationship, the primer may selectively dampen aspects of A that don't align well with token C's instantaneous but noisy correlation with A. As such, prime attention's representational plasticity in pair-wise relational modeling allows for richer, more effective pattern discovery as tokens become better aligned to capture the unique dynamics within each pair.

Our proposed prime attention maintains the asymptotic computational complexity of standard attention while providing transformers with the representational flexibility needed to capture rich, heterogeneous pair-wise dynamics that standard attention struggles with in MTS. Our empirical results in Section 7 show that prime attention consistently outperforms standard attention on state-of-the-art MTS transformers across benchmarks, achieving up to 6.5% improvement in forecasting accuracy. We also show that prime attention, in certain instances, can use up to 40% less sequence length while achieving comparable (or slightly better) performance than standard attention, empirically demonstrating prime attention's superior relational modeling capabilities. We also comapre prime attention against a selection of recent works in MTS that perform sophisticated relational learning beyond standard attention and find that prime attention consistently outperforms them as well.

2 Related Works

Recent advances in MTS forecasting have demonstrated important progress toward relational modeling strategies. iTransformer (Liu et al., 2024) represents among the most performant transformers that explicitly model channel-wise relationships. Timer-XL (Liu et al., 2025b) similarly captures inter-channel dependencies using a transformer. FreDF (Wang et al., 2025) uses a standard channel-wise transformer as a backbone but also considers model optimization in the frequency domain. Adjacent to channel-wise transformers, patch-based transformers (Zhang & Yan, 2023; Wang et al., 2024d) have also been successful in modeling inter-channel dependencies, tokenizing segments within each channel for more fine-grained interactions. While these methods have shown robust performance, their unifying limitation lies in their static relational modeling. There also exist works that avoid inter-channel interactions entirely, opting for a channel-independent (CI) approach. More information on CI models can be found in Appendix B.

Some recent works capture specific types of inter-channel relationships in more explicit ways. LIFT (Zhao & Shen, 2024) explicitly estimates lead-lag patterns between channels during pre-processing while LagTS (Liu et al., 2025a) represents a more unified approach, integrating lead-lag estimation into the learning process. LagTS first extracts relational information between pairs of channels through an MLP and employs a custom loss function to guide the learning of lagged correlations. However, this approach remains fundamentally constrained by the static relational learning paradigm where channel representations remain invariant across all pair-wise interactions within each layer. Channel Clustering Module (CCM) (Chen et al., 2024) addresses relationship heterogeneity by employing learnable similarity metrics to group compatible channels, enabling cluster-specific processing that can capture shared patterns within channel groups. However, CCM's group-level processing potentially limits their ability to model unique dynamics between individual channel pairs that don't conform to cluster-wide patterns. Overall, while these approaches represent significant advances in relationship-aware modeling for MTS, they are architecturally constrained by their design focus on specific categories of inter-channel dependencies and static relational learning.

3 Enhancing Attention by Sharpening the Coefficients

Recent advances in attention mechanisms have increasingly focused on selective modulation of attention components to improve relational learning. However, current attention enhancement strategies are often fundamentally constrained by their sole focus on modulating attention coefficients. The differential transformer (Ye et al., 2025) subtracts the learned attention map with another, denoising, attention map to systematically reduce noise accumulation and improve focus on relevant context. Selective attention (Leviathan et al., 2025) uses a learnable mask on the attention map to achieve similar results. Likewise, a recent theoretical study on softmax function has formalized such enhancement strategies and proposes a way to adaptively enhance attention coefficients as a potential solution (Veličković et al., 2025).

While enhancing attention coefficients by modulating the attention map has shown to improve performance and reduce noise accumulation particularly in the language domain, they still use static tokens to improve their attention coefficients. As such, they can broadly be seen as instances of standard attention with *sharpened* attention scores, certainly improving upon standard attention but still fundamentally constrained by the static relational learning paradigm as further explored in the next section.

4 Categorizing Relational Learning

Here, we formalize static and dynamic relational learning. We broadly refer to relational learning as methodologies that explicitly model interactions and dependencies between discrete entities in structured data, such as tokens in a set, nodes in a graph, or channels in MTS. In particular, we focus on dyadic, or pair-wise, relational learning.

Formally, given a set of entities $\mathcal{X} = \{x_1, x_2, ..., x_N\},\ \ x_i \in \mathbb{R}^d$, we define relational learning broadly as seeking to capture the interaction function $f(x_i, x_j) \rightarrow \mathbb{R}^d$ that characterizes the dependency between each pair (x_i, x_j) for which i and j have some computational relationship. Our question of interest in relational learning is how the core representations of entities $(x_i, x_j)\ \forall i, j \in \{1, ..., N\}$ are conditioned during pairwise interactions in f.

Definition 4.1 (Static relational learning)**.** *For any valid pair of entities (x_i, x_j), the relational learning process f is* **static** *if representations of x_i and x_j are invariant to each other.*

Formally, for any pair (x_i, x_j), the representations used in interaction are:

$$h_{i \to j} = \psi(x_i; \theta_i), \quad h_{j \to i} = \psi(x_j; \theta_j) \tag{1}$$

where $h_{i \to j}$ can be interpreted as representation of x_i created for interaction with x_j and vice versa. Then, the relational learning process is static if $\psi(\cdot; \theta_n)$ is independent of the interaction partner which results in $h_{j \to n} = h_{j \to i},\ \forall n \in \{1, .., N\}$ for any particular i and j in each layer.

Definition 4.2 (Dynamic relational learning)**.** *For any valid pair of entities (x_i, x_j), the relational learning process f is* ***dynamic*** *if representation of x_j can dynamically adapt for x_i based on some computational or optimization criteria.*

Formally, for any pair (x_i, x_j), their representations in dynamic relational learning are:

$$h_{i \to j} = \psi(x_i; \theta_i), \quad h_{j \to i} = \psi(x_j; \theta_j, \phi_{ij}) \tag{2}$$

where ϕ_{ij} explicitly conditions the representation of x_j on pair-specific (x_i, x_j) dynamics and θ_j represents pair-invariant parameters for x_j. Thus, under dynamic relational learning, $h_{j \to n}$ is not constrained to be equal to $h_{j \to i},\ \forall n \in \{1, ..., N\}, n \neq i$.

With the following characterizations, we can show that attention mechanism in transformers perform static relational learning.

Theorem 4.3. *Standard attention in transformers implements static relational learning.*

Proof. In standard attention, relational modeling between any two tokens (x_i, x_j) can be defined as:

$$f(x_i, x_j) = \alpha_{ii} \cdot h_{i \to j} + \alpha_{ij} \cdot h_{j \to i} \tag{3}$$

$$\alpha_{ii} = e(h_{i \to j}, h_{i \to j}), \quad \alpha_{ij} = e(h_{i \to j}, h_{j \to i}) \tag{4}$$

where $e(\cdot) \to \mathbb{R}$ is the (possibly learnable) attention scoring function typically defined as an inner product. Representations $h_{i \to j}$ and $h_{j \to i}$ are computed as follows:

$$h_{i \to j} = x_i W_q \tag{5}$$

$$h_{j \to i} = x_j W_{kv} \tag{6}$$

where $W_q, W_{kv} \in \mathbb{R}^{d \times d_{model}}$ are learned projection matrices. Then, entity representations for relational learning $f(x_u, x_j)$ for any $u \neq i$ is formulated as:

$$h_{u \to j} = x_u W_q \tag{7}$$

$$h_{j \to u} = x_j W_{kv} \tag{8}$$

where $h_{j \to u} = h_{j \to i} = x_j W_{kv},\ \forall u \in \{1, ..., N\}$. Therefore, standard attention computes static relational learning. *Note: while we simplify the key-value projections for notational clarity and to visually emphasize pair-wise dynamics, having separate key and value projections do not change our theoretical framework or its conclusions.*

As a consequence of Theorem 4.3, no amount of *sharpening* of attention coefficients α can alleviate the static nature of relational learning in standard attention. This also extends to other forms of possibly multi-dimensional relational information such as edge-features in some GNNs as long as the underlying representations that formulate such relational information are static.

5 Attention with Dynamic Relational Priming

Having established an understanding of our categorization of relational learning, we now introduce our proposed methodology. We first show how standard attention is modified to enable prime attention. Next, we discuss how the learnable primers are constructed through which pair-wise priming of tokens occur. Finally, we show how prime attention enables dynamic relational learning to overcome the limitations of standard attention in MTS.

Prime Attention for Transformers Mathematically, given tokens $x_i, x_j \in \mathbb{R}^{d_{token}}$ for some $i, j \in \{1, ..., N\}$ where N denotes the number of tokens, the query vector $q_i = x_i W_q$ and key, value vectors $k_j = x_j W_k$, $v_j = x_j W_v$ are derived with projection matrices $W_q, W_k, W_v \in \mathbb{R}^{d_{token} \times d_{model}}$. Then, standard attention computation for token x_i is defined as:

$$x_i' = \sum_{j=1}^{N} softmax_j(e(q_i, k_j))v_j \tag{9}$$

where $e(\cdot)$ represents some pair-wise scoring function such as an inner product. We have established in Theorem 4.3 how this formulation results in static relational learning.

On the other hand, prime attention enables each token to present dynamically primed perspective of itself based on the specific token-pair context. This is achieved as:

$$\widetilde{x}_i' = \sum_{j=1}^{N} softmax_j(e(q_i, \widetilde{k}_j))\widetilde{v}_j \tag{10}$$

where $\widetilde{k}_j$ and $\widetilde{v}_j$ are defined as:

$$\widetilde{k}_j = k_j \odot \mathcal{F}_{i,j} \tag{11}$$

$$\widetilde{v}_j = v_j \odot \mathcal{F}_{i,j} \tag{12}$$

where $\odot$ represents element-wise multiplication and $\mathcal{F}_{i,j} \in \mathbb{R}^{d_{model}}$ represents a learnable primer designed to give pair-wise relational context to token-pair x_i and x_j. The primer $\mathcal{F}_{i,j}$ can learn to amplify or dampen different portions of the token representation to make certain relationship discoveries easier. As such, $\widetilde{k}_j$ and $\widetilde{v}_j$ are updated versions of k_j and v_j modulated specifically to maximize relevant information extraction from that particular token-pair (x_i-x_j). For example, $\mathcal{F}_{i,j}$ might modulate k_j and v_j to make lead-lag correlations more easily discoverable if the model learns that such relationship exists between tokens i and j. For a different pair x_k and x_j, $\mathcal{F}_{k,j}$ may amplify and dampen certain parts of k_j and v_j to make instantaneous couplings more easily discoverable instead.

Learnable Modulator Generation The primer $\mathcal{F}_{i,j}$ can be learned from scratch (with random initialization near the identity I) or expanded, in a learnable fashion, from estimated known patterns that exist in the domain (like lead-lag relationships and other temporal dynamics). In the simplest case, $\mathcal{F}_{i,j}$ can be constructed from some random initialization $s \sim \mathcal{N}_{d_{model}}(\mu, \Sigma)$ and made learnable through a neural network, such as $\mathcal{F}_{i,j} = MLP(s_{ij})$.

To potentially accelerate the discovery of patterns that are known to exist in the given data, s can be initialized with estimations of such known patterns. An example of such pattern in MTS is lead-lag correlations that exist between channels. Following from Zhao & Shen (2024), lead-lag coefficients between channels x_i and x_j for all possible leading steps $\{1, ..., \mathcal{L}\}$ within a look-back window $L = \{t - \mathcal{L} + 1 : t\}$ can be calculated as follows:

$$\{R_{i,j}^{(t)}(\tau)\}_{\tau=1}^{\mathcal{L}} = \frac{1}{\mathcal{L}} \mathcal{FFT}^{-1}(\mathcal{FFT}(x_j^L) \odot \mathcal{FFT}_{conj}(x_i^L)) \tag{13}$$

where $\mathcal{FFT}(\cdot)$ denotes the fast fourier transform and x_i^L denotes the look-back window L of channel i.

Then, the initialization can be biased with $\widetilde{s_{ij}} = \sigma(R_{i,j}^{(t)})W$ where $W \in \mathbb{R}^{\mathcal{L} \times d_{model}}$ represents some learnable projection matrix and the optional $\sigma(\cdot)$ can be a smoothing function such as $tanh(\cdot)$ used to normalize and smooth-out the raw values of $R_{i,j}^{(t)}$. The filter $\mathcal{F}_{i,j} = MLP(\widetilde{s_{ij}})$ can then learn to selectively amplify or dampen the introduced pattern information through the learnable neural network, $MLP(\cdot)$. While lead-lag is a one example of a relational pattern that may exist in MTS data, other information (such as instantaneous correlation, non-linear coupling, etc.) can also be used in conjunction to allow the MLP to learn which known possible patterns are the most effective for each relationship dynamic.

Dynamic Relational Learning with Prime Attention Here we show how prime attention enables dynamic relational learning, providing the representational adaptability crucial for capturing heterogeneous relational patterns characteristic of MTS systems.

Theorem 5.1. *Prime attention enables dynamic relational learning in transformers.*

Proof. In prime attention, relational modeling between any two entities (x_i, x_j) can be defined as:

$$f(x_i, x_j) = \alpha_{ii} \cdot h_{i \to j} + \alpha_{ij} \cdot \widetilde{h}_{j \to i} \tag{14}$$

$$\alpha_{ii} = e(h_{i \to j}, h_{i \to j}), \quad \alpha_{ij} = e(h_{i \to j}, \widetilde{h}_{j \to i}) \tag{15}$$

where entity representation $h_{i \to j}$ and $\widetilde{h}_{j \to i}$ are derived as:

$$\widetilde{h}_{j \to i} = h_{j \to i} \odot \mathcal{F}_{ji} \tag{16}$$

$$h_{i \to j} = x_i W_q, \quad h_{j \to i} = x_j W_{kv} \tag{17}$$

where $W_q, W_{kv} \in \mathbb{R}^{d \times d_{model}}$ are learned projection matrices. Then, relational learning $f(x_v, x_j)$ for any $v \neq i$ is formulated as:

$$f(x_v, x_j) = \alpha_{vv} \cdot h_{v \to j} + \alpha_{vj} \cdot \widetilde{h}_{j \to v} \tag{18}$$

and it can be seen that:

$$\widetilde{h}_{j \to i} = x_j W_{kv} \odot \mathcal{F}_{ji} \tag{19}$$

$$\widetilde{h}_{j \to v} = x_j W_{kv} \odot \mathcal{F}_{jv} \tag{20}$$

and since $\mathcal{F}_{ji}$ and $\mathcal{F}_{jv}$ are independent learnable parameters, they are not constrained to be equal. In general, after training, $\mathcal{F}_{ji} \neq \mathcal{F}_{jv}$ for $v \neq i.$ As a result, $\widetilde{h}_{j \to v} \neq \widetilde{h}_{j \to i}$ for $v \neq i.$ Therefore, prime attention performs dynamic relational learning where entities can dynamically adapt to each pair-wise interaction.

As a consequence of Theorem 5.1, the representational plasticity of prime attention's dynamic relational learning allows each token to present computationally optimized perspectives for different interaction partners. In domains like MTS where there can be high degrees of relational heterogeneity between different pair-wise interactions, prime attention's dynamic relational learning can allow robust discovery of different patterns for different pair-wise relationships. In addition, we show that prime attention, much like standard attention, satisfies the universal approximation theorem in Appendix E and provide a gradient flow analysis for prime attention in Appendix F.

Complexity Analysis Overall, prime attention introduces controlled computational overhead while preserving asymptotic computational complexity of standard attention. The core additional cost stems from the learnable primer $\mathcal{F} \in \mathbb{R}^{N^2 \times d_{model}}$ where N is typically the number of channels, which requires $\mathcal{O}(N^2 \times d_{model})$ memory storage and introduces element-wise multiplication operations for both key and value modulation during attention computation. While this approximately doubles the floating-point operations compared to standard attention, the overall computational complexity remains unchanged. The memory overhead scales quadratically with N, which is manageable for typical MTS applications where number of channels are under 1000.

However, the memory requirements of prime attention can become problematic for higher-dimensional systems. Likewise, depending on the MTS system, not every pair-wise interaction may need a dedicated primer. Therefore, we introduce a graph neural network (GNN) based sparsification strategy in Appendix D.2 as one example of how prime attention can be adapted for resource efficiency and topological alignment, achieving $O(|E| \times d_{model})$ where $|E| \ll N^2$.

6 Universal Approximation and Inductive Biases

Prime attention's dynamic relational learning mechanism can be seen as an instance of learnable inductive bias injected into every pair-wise relationship in attention mechanism. Viewing prime attention through this lens allows us to make strong justifications about why prime attention can enable superior relational modeling capabilities compared to standard attention despite standard attention's universal approximation guarantees.

While transformers with standard attention theoretically satisfy universal approximation guarantees (Cybenko, 1989; Yun et al., 2020) and can model any relationship pattern given sufficient depth, width, and training data, practical constraints make these theoretical capabilities largely inaccessible. In this constrained regime, appropriate inductive biases have shown success in directing model capacity toward learning meaningful patterns efficiently. *Note: we show in Appendix E that prime attention also satisfies universal approximation theorem.*

Inductive biases are prior assumptions a model holds that influence its ability to generalize to new, unseen data. Simply put, inductive biases serve to nudge the model learning process towards directions where useful learning is more likely to occur. In graph representation learning, the presence of edges serves to inductively bias the model towards discovering topologically relevant patterns (Hamilton et al., 2017; Gilmer et al., 2017). In geometric GNNs, inductively biasing the model through invariant or equivariant computations have shown tremendous success in molecular modeling, allowing for faster model convergence while using dramatically fewer data samples during training (Vignac et al., 2020; Joshi et al., 2023; Batzner et al., 2022). Even positional encoding in transformers (Vaswani et al., 2017; Su et al., 2024; Barbero et al., 2025) can be seen as inductively biasing the model with explicit assumptions of sequential structure and distance information of tokens. Overall, inductive biases typically don't expand what the model can theoretically represent. However, by biasing the model through assumptions and contextually relevant information, it can dramatically improve what the model can learn efficiently with limited data and model capacity.

Dynamic priming of tokens through learned primers $\mathcal{F}$ for each pair-wise interaction can be seen as an instance of dynamic and learnable inductive bias for the attention mechanism. Whether learned from scratch or initialized from known estimated patterns, $\mathcal{F}$ serves to bias the relational learning process to discover useful pair-wise dynamics. By inductively biasing pair-wise relationships, prime attention can enable faster and more reliable discoveries of different patterns that exist between channels. This can be particularly beneficial in MTS systems with high degrees of channel heterogeneity. Prime attention's ability to achieve comparable performance while using only a fraction of the sequence length used in standard attention (as shown in Section 7) aligns well with observed benefits of inductive bias in other domains and present notable positive implications for MTS modeling in data-scarce systems.

7 Experiments

Experimental Setup We use 11 widely-acknowledged benchmark datasets in our experiments made up of 9 long-term and 2 short-term datasets. These include Weather (Wu et al., 2021), Solar (Lai et al., 2018), Traffic (Wu et al., 2021) and more. More information on the datasets can be found in Appendix A.1 and experimental details can be found in Appendix A.2.

7.1 Forecasting Evaluation

For the main forecasting benchmarks, we fix the look-back window length at $L = 96$ and predict on horizon values $H \in \{96, 192, 336, 720\}$ except for the PEMS data where $H \in \{12, 24, 48, 96\}$. We also provide the averaged performance across all horizons.

We use 3 state-of-the-art MTS transformers–Timer-XL (Liu et al., 2025b), FreDF (Wang et al., 2025), and iTransformer (Liu et al., 2024)–as backbone architectures to compare prime and standard attention in MTS forecasting. The prime attention version of these transformers are obtained by simply swapping out the main attention block with prime attention changing nothing else and keeping with the original hyper-parameters except dropout. The results are shown in Table 1. For each architecture, forecasting accuracy of standard and prime attention are recorded side-by-side with better performance in each model colored in **teal** if prime attention is better and in **brown** if standard attention is better. We use the abridged version here and the full table is available in Appendix H, Table 6. We observe consistent performance improvements using prime attention across datasets and models. On datasets with heterogeneous channels such as Solar and Weather where different channels record different physical properties, we observe average improvement across models of up to 4.0% when using prime attention. Specifically, prime attention shows a 6.5% improvement against standard attention on Weather dataset using Timer-XL. On the other hand, on ECL and Traffic where all channels record the same attribute (i.e. electric consumption and traffic flow, respectively), prime attention's performance gains were marginal. This aligns well with our hypothesized benefits of prime attention and show that in cases where channel relationships are relatively homogenous, standard attention is still capable of robust performance. On short-term forecasts, prime attention achieved an average performance gain of 5.5%, indicating its ability to accurately capture noisy short-term patterns that standard attention struggles with.

Table 1: Comparison between standard attention and prime attention on recent state-of-the-art transformer models (abridged). Lower values indicate better performance. Full table is available in Appendix H, Table 6.

Model		Timer-XL (2025)				FreDF (2025)				iTransformer (2024)			
Attn Type		Standard		***Prime***		Standard		***Prime***		Standard		***Prime***	
		MSE	MAE	MSE	MAE	MSE	MAE	MSE	MAE	MSE	MAE	MSE	MAE
ETTh1	Avg.	0.453	0.445	**0.438**	**0.435**	0.452	0.443	**0.449**	**0.441**	0.449	0.443	**0.440**	**0.438**
ETTh2	Avg.	0.396	0.415	**0.389**	**0.412**	0.390	0.411	**0.389**	**0.409**	0.385	0.409	**0.377**	**0.404**
ETTm1	Avg.	0.441	0.428	**0.427**	**0.420**	0.402	**0.402**	**0.400**	0.402	0.405	0.409	**0.394**	**0.404**
ETTm2	Avg.	0.293	0.334	**0.290**	**0.332**	**0.289**	**0.327**	0.289	0.327	0.287	0.331	**0.282**	**0.327**
Weather	Avg.	0.277	0.311	**0.259**	**0.282**	0.262	0.279	**0.256**	**0.276**	0.261	0.281	**0.254**	**0.277**
Solar-Energy	Avg.	0.282	**0.284**	**0.279**	0.285	0.234	0.254	**0.229**	**0.251**	0.238	0.265	**0.229**	**0.258**
ECL	Avg.	0.179	0.273	**0.176**	**0.268**	0.169	0.260	**0.168**	**0.258**	**0.174**	0.267	0.175	**0.266**
Traffic	Avg.	0.443	**0.288**	**0.436**	0.289	0.428	0.276	**0.424**	**0.274**	0.430	0.282	**0.426**	**0.280**
PEMS03	Avg.	-	-	-	-	0.138	0.242	**0.133**	**0.237**	0.142	0.248	**0.139**	**0.243**
PEMS08	Avg.	-	-	-	-	0.172	0.250	**0.161**	**0.241**	0.183	0.263	**0.167**	**0.248**

In addition, we also compare prime attention against a selection of MTS architectures that perform sophisticated relational learning beyond standard attention. These include LagTS (Liu et al., 2025a) and LIFT (Zhao & Shen, 2024) as well as our implementation of the differential transformer (DIFF transformer) (Ye et al., 2025) using iTransformer (Liu et al., 2024) as backbone. We also include Autoformer (Wu et al., 2021), an earlier but seminal work in MTS transformers that replaces standard attention with an auto-correlation mechanism for better pattern discovery. Their abridged results are reported in Table 2, where prime attention continues to exhibit superior performance in the majority of instances. The best results in each dataset are shown in **teal**. The unabridged, full table is available in Appendix H, Table 5.

Table 2: Performance comparison between prime attention and existing works in MTS that enhance and leverage relational information (abridged). Lower values indicate better performance. Full table is available in Appendix H, Table 5.

Model		***Prime Attn.* (Ours)**		DIFF Transformer (2025)		LagTS (2025)		LIFT (2024)		Autoformer (2021)	
Metrics		MSE	MAE	MSE	MAE	MSE	MAE	MSE	MAE	MSE	MAE
ETTh1	Avg.	0.440	**0.438**	0.446	0.440	**0.439**	0.439	0.443	0.439	0.496	0.487
ETTh2	Avg.	**0.377**	**0.404**	0.386	0.411	0.382	0.405	0.386	0.408	0.450	0.459
Exchange	Avg.	**0.339**	**0.392**	0.357	0.401	0.341	0.397	0.356	0.403	0.613	0.539
Weather	Avg.	**0.254**	**0.277**	0.259	0.280	0.258	0.281	0.260	0.282	0.338	0.382

7.2 Sequence Length Efficiency Analysis

Here, we perform a sequence length (or look-back window length L) analysis for standard and prime attention. Namely, we are interested in seeing how performance improves with longer sequence length (or more input data). Performance for each model is measured across $L \in \{16, 32, 48, 64, 80, 96\}$ and the prediction horizon is fixed at $H = 96$. We show the results in Figure 1, using iTransformer Liu et al. (2024) as backbone for both standard and prime attention.

Remarkably, prime attention not only shows improved performance at each L as expected, but it also shows that it can match or slightly outperform standard attention's performance with significantly less input sequence length in some instances. To illustrate this, we use a horizontal green dotted line labeled *target threshold* to mark the performance of standard attention when using $L = 96$. As shown in Figures 1a and 1b, prime attention breaks through the target threshold using sequence lengths of 48 and 64, which translates to using 40% and 33% less input data compared to standard attention, respectively. We show in Appendix G.2 how this can translate to prime attention exhibiting lower *effective* complexity than standard attention by requiring less data to reduce overhead while maintaining superior performance. While such significant results were not observed across all datasets, it does align well with the observed benefits of inductive biases in other domains. It also strengthens our argument from Section 6 that prime attention acts as a learnable inductive bias in attention to enable and accelerate effective discoveries of unique relational dynamics across pair-wise interactions. In addition, this finding may be of interest in domains where input data is scarce. We provide additional results in Appendix G.4.

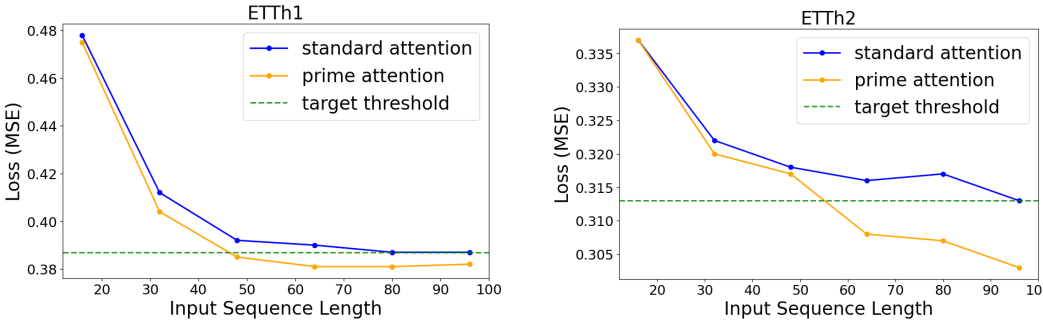

(a)

(b)

Figure 1: Comparing performance between standard (blue) and prime (yellow) attention at various input sequence length (or look-back window L). The horizontal target threshold line (green, dotted) represents standard attention's performance at $L = 96$. Lower values indicate better performance.

7.3 Additional Analysis

We perform ablation studies in Appendix G.1 to study the effects of sparsity and initialization strategies in designing the learnable modulator $\mathcal{F}$. Complexity analysis is done in Appendix G.2 where we show that prime attention can exhibit lower *effective* complexity than standard attention. In addition, we perform an attention map analysis in Appendix G.3 for both standard and prime attention and uncover that prime attention is potent enough to act as a hybrid CD/CI model in certain instances.

8 Conclusion

We introduced prime attention, a novel attention mechanism enabling dynamic relational learning through pair-wise token modulation for multivariate time series (MTS) forecasting. Unlike standard attention's static relational learning, prime attention dynamically adapts token representations for each specific interaction via learnable primers, better capturing the heterogeneous inter-channel dependencies characteristic of many MTS systems. Our results show that prime attention consistently outperforms standard attention and demonstrate the practical benefits of dynamic relational learning in MTS. We discuss limitations and future work in Appendix C.

Reproducibility Statement

We describe in detail our proposed methodology in Section 5 and appendix D.2, make available the experimental settings in Appendix A.2, and release our code with detailed instructions to reproduce our results independently. In addition, we provide clear proofs and assumptions for all of our theoretical results.

References

Josh Achiam, Steven Adler, Sandhini Agarwal, Lama Ahmad, Ilge Akkaya, Florencia Leoni Aleman, Diogo Almeida, Janko Altenschmidt, Sam Altman, Shyamal Anadkat, et al. Gpt-4 technical report. *arXiv preprint arXiv:2303.08774*, 2023.

Dzmitry Bahdanau, Kyunghyun Cho, and Yoshua Bengio. Neural machine translation by jointly learning to align and translate. *arXiv preprint arXiv:1409.0473*, 2014.

Federico Barbero, Alex Vitvitskyi, Christos Perivolaropoulos, Razvan Pascanu, and Petar Veličković. Round and round we go! what makes rotary positional encodings useful? In *The Thirteenth International Conference on Learning Representations*, 2025. URL `https://openreview.net/forum?id=GtvuNrk58a`.

Simon Batzner, Albert Musaelian, Lixin Sun, Mario Geiger, Jonathan P Mailoa, Mordechai Kornbluth, Nicola Molinari, Tess E Smidt, and Boris Kozinsky. E (3)-equivariant graph neural networks for data-efficient and accurate interatomic potentials. *Nature communications*, 13(1): 2453, 2022.

Shaked Brody, Uri Alon, and Eran Yahav. How attentive are graph attention networks? *arXiv preprint arXiv:2105.14491*, 2021.

Nicolas Carion, Francisco Massa, Gabriel Synnaeve, Nicolas Usunier, Alexander Kirillov, and Sergey Zagoruyko. End-to-end object detection with transformers. In *European conference on computer vision*, pp. 213–229. Springer, 2020.

Hui Chen, Viet Luong, Lopamudra Mukherjee, and Vikas Singh. SimpleTM: A simple baseline for multivariate time series forecasting. In *The Thirteenth International Conference on Learning Representations*, 2025. URL `https://openreview.net/forum?id=oANkBaVci5`.

Jialin Chen, Jan Eric Lenssen, Aosong Feng, Weihua Hu, Matthias Fey, Leandros Tassiulas, Jure Leskovec, and Rex Ying. From similarity to superiority: Channel clustering for time series forecasting. *Advances in Neural Information Processing Systems*, 37:130635–130663, 2024.

Si-An Chen, Chun-Liang Li, Nate Yoder, Sercan O Arik, and Tomas Pfister. Tsmixer: An all-mlp architecture for time series forecasting. *arXiv preprint arXiv:2303.06053*, 2023.

George V. Cybenko. Approximation by superpositions of a sigmoidal function. *Mathematics of Control, Signals and Systems*, 2:303–314, 1989. URL `https://api.semanticscholar.org/CorpusID:3958369`.

Andreea Deac, Marc Lackenby, and Petar Veličković. Expander graph propagation. In *Learning on Graphs Conference*, pp. 38–1. PMLR, 2022.

Jacob Devlin, Ming-Wei Chang, Kenton Lee, and Kristina Toutanova. Bert: Pre-training of deep bidirectional transformers for language understanding. In *Proceedings of the 2019 conference of the North American chapter of the association for computational linguistics: human language technologies, volume 1 (long and short papers)*, pp. 4171–4186, 2019.

Alexey Dosovitskiy, Lucas Beyer, Alexander Kolesnikov, Dirk Weissenborn, Xiaohua Zhai, Thomas Unterthiner, Mostafa Dehghani, Matthias Minderer, Georg Heigold, Sylvain Gelly, et al. An image is worth 16x16 words: Transformers for image recognition at scale. *arXiv preprint arXiv:2010.11929*, 2020.

Justin Gilmer, Samuel S Schoenholz, Patrick F Riley, Oriol Vinyals, and George E Dahl. Neural message passing for quantum chemistry. In *International conference on machine learning*, pp. 1263–1272. Pmlr, 2017.

Xavier Glorot and Yoshua Bengio. Understanding the difficulty of training deep feedforward neural networks. In Yee Whye Teh and Mike Titterington (eds.), *Proceedings of the Thirteenth International Conference on Artificial Intelligence and Statistics*, volume 9 of *Proceedings of Machine Learning Research*, pp. 249–256, Chia Laguna Resort, Sardinia, Italy, 13–15 May 2010. PMLR. URL https://proceedings.mlr.press/v9/glorot10a.html.

Meng-Hao Guo, Tian-Xing Xu, Jiang-Jiang Liu, Zheng-Ning Liu, Peng-Tao Jiang, Tai-Jiang Mu, Song-Hai Zhang, Ralph R Martin, Ming-Ming Cheng, and Shi-Min Hu. Attention mechanisms in computer vision: A survey. *Computational visual media*, 8(3):331–368, 2022.

Will Hamilton, Zhitao Ying, and Jure Leskovec. Inductive representation learning on large graphs. *Advances in neural information processing systems*, 30, 2017.

William L Hamilton. *Graph representation learning*. Morgan & Claypool Publishers, 2020.

Lu Han, Han-Jia Ye, and De-Chuan Zhan. The capacity and robustness trade-off: Revisiting the channel independent strategy for multivariate time series forecasting. *IEEE Transactions on Knowledge and Data Engineering*, 36(11):7129–7142, 2024.

Ziniu Hu, Yuxiao Dong, Kuansan Wang, and Yizhou Sun. Heterogeneous graph transformer. In *Proceedings of the web conference 2020*, pp. 2704–2710, 2020.

Chaitanya K Joshi. Transformers are graph neural networks. *arXiv preprint arXiv:2506.22084*, 2025.

Chaitanya K Joshi, Cristian Bodnar, Simon V Mathis, Taco Cohen, and Pietro Lio. On the expressive power of geometric graph neural networks. In *International conference on machine learning*, pp. 15330–15355. PMLR, 2023.

Taesung Kim, Jinhee Kim, Yunwon Tae, Cheonbok Park, Jang-Ho Choi, and Jaegul Choo. Reversible instance normalization for accurate time-series forecasting against distribution shift. In *International Conference on Learning Representations*, 2022. URL https://openreview.net/forum?id=cGDAkQo1C0p.

Diederik P Kingma and Jimmy Ba. Adam: A method for stochastic optimization. *arXiv preprint arXiv:1412.6980*, 2014.

TN Kipf. Semi-supervised classification with graph convolutional networks. *arXiv preprint arXiv:1609.02907*, 2016.

Guokun Lai, Wei-Cheng Chang, Yiming Yang, and Hanxiao Liu. Modeling long-and short-term temporal patterns with deep neural networks. In *The 41st international ACM SIGIR conference on research & development in information retrieval*, pp. 95–104, 2018.

Yaniv Leviathan, Matan Kalman, and Yossi Matias. Selective attention improves transformer. In *The Thirteenth International Conference on Learning Representations*, 2025. URL https://openreview.net/forum?id=v0FzmPCd1e.

Ciyi Liu, Jiaqi Ye, Zhenpeng Yu, Shubao Zhao, Zhaoxiang Hou, Chengyi Yang, Yanlong Wen, and Xiaojie Yuan. Lagts: Toward adaptive lag relationship modeling for multivariate time series forecasting. In *ICASSP 2025 - 2025 IEEE International Conference on Acoustics, Speech and Signal Processing (ICASSP)*, pp. 1–5, 2025a. doi: 10.1109/ICASSP49660.2025.10890275.

Yong Liu, Haixu Wu, Jianmin Wang, and Mingsheng Long. Non-stationary transformers: Exploring the stationarity in time series forecasting. *Advances in neural information processing systems*, 35: 9881–9893, 2022.

Yong Liu, Tengge Hu, Haoran Zhang, Haixu Wu, Shiyu Wang, Lintao Ma, and Mingsheng Long. itransformer: Inverted transformers are effective for time series forecasting. In *The Twelfth International Conference on Learning Representations*, 2024. URL https://openreview.net/forum?id=JePfAI8fah.

Yong Liu, Guo Qin, Xiangdong Huang, Jianmin Wang, and Mingsheng Long. Timer-XL: Long-context transformers for unified time series forecasting. In *The Thirteenth International Conference on Learning Representations*, 2025b. URL https://openreview.net/forum?id=KMCJXjlDDr.

Yuqi Nie, Nam H Nguyen, Phanwadee Sinthong, and Jayant Kalagnanam. A time series is worth 64 words: Long-term forecasting with transformers. *arXiv preprint arXiv:2211.14730*, 2022.

Adam Paszke, Sam Gross, Francisco Massa, Adam Lerer, James Bradbury, Gregory Chanan, Trevor Killeen, Zeming Lin, Natalia Gimelshein, Luca Antiga, et al. Pytorch: An imperative style, high-performance deep learning library. *Advances in neural information processing systems*, 32, 2019.

Xiangfei Qiu, Hanyin Cheng, Xingjian Wu, Jilin Hu, Chenjuan Guo, and Bin Yang. A comprehensive survey of deep learning for multivariate time series forecasting: A channel strategy perspective. *arXiv preprint arXiv:2502.10721*, 2025.

Ladislav Rampášek, Michael Galkin, Vijay Prakash Dwivedi, Anh Tuan Luu, Guy Wolf, and Dominique Beaini. Recipe for a general, powerful, scalable graph transformer. *Advances in Neural Information Processing Systems*, 35:14501–14515, 2022.

Michael Schlichtkrull, Thomas N Kipf, Peter Bloem, Rianne Van Den Berg, Ivan Titov, and Max Welling. Modeling relational data with graph convolutional networks. In *European semantic web conference*, pp. 593–607. Springer, 2018.

Jianlin Su, Murtadha Ahmed, Yu Lu, Shengfeng Pan, Wen Bo, and Yunfeng Liu. Roformer: Enhanced transformer with rotary position embedding. *Neurocomputing*, 568:127063, 2024.

Ashish Vaswani, Noam Shazeer, Niki Parmar, Jakob Uszkoreit, Llion Jones, Aidan N Gomez, Łukasz Kaiser, and Illia Polosukhin. Attention is all you need. *Advances in neural information processing systems*, 30, 2017.

Petar Veličković, Guillem Cucurull, Arantxa Casanova, Adriana Romero, Pietro Lio, and Yoshua Bengio. Graph attention networks. *arXiv preprint arXiv:1710.10903*, 2017.

Petar Veličković, Christos Perivolaropoulos, Federico Barbero, and Razvan Pascanu. softmax is not enough (for sharp out-of-distribution), 2025. URL https://openreview.net/forum?id=wMj6PgKVuJ.

Clement Vignac, Andreas Loukas, and Pascal Frossard. Building powerful and equivariant graph neural networks with structural message-passing. *Advances in neural information processing systems*, 33:14143–14155, 2020.

Hao Wang, Lichen Pan, Yuan Shen, Zhichao Chen, Degui Yang, Yifei Yang, Sen Zhang, Xinggao Liu, Haoxuan Li, and Dacheng Tao. FreDF: Learning to forecast in the frequency domain. In *The Thirteenth International Conference on Learning Representations*, 2025. URL https://openreview.net/forum?id=4A9IdSa1ul.

Shiyu Wang, Jiawei Li, Xiaoming Shi, Zhou Ye, Baichuan Mo, Wenze Lin, Shengtong Ju, Zhixuan Chu, and Ming Jin. Timemixer++: A general time series pattern machine for universal predictive analysis. *arXiv preprint arXiv:2410.16032*, 2024a.

Shiyu Wang, Haixu Wu, Xiaoming Shi, Tengge Hu, Huakun Luo, Lintao Ma, James Y Zhang, and JUN ZHOU. Timemixer: Decomposable multiscale mixing for time series forecasting. In *International Conference on Learning Representations (ICLR)*, 2024b.

Shiyu Wang, Haixu Wu, Xiaoming Shi, Tengge Hu, Huakun Luo, Lintao Ma, James Y Zhang, and Jun Zhou. Timemixer: Decomposable multiscale mixing for time series forecasting. *arXiv preprint arXiv:2405.14616*, 2024c.

Xiao Wang, Houye Ji, Chuan Shi, Bai Wang, Yanfang Ye, Peng Cui, and Philip S Yu. Heterogeneous graph attention network. In *The world wide web conference*, pp. 2022–2032, 2019.

Yuxuan Wang, Haixu Wu, Jiaxiang Dong, Guo Qin, Haoran Zhang, Yong Liu, Yunzhong Qiu, Jianmin Wang, and Mingsheng Long. Timexer: Empowering transformers for time series forecasting with exogenous variables. *Advances in Neural Information Processing Systems*, 37:469–498, 2024d.

JJ Wilson, Maya Bechler-Speicher, and Petar Veličković. Cayley graph propagation. *arXiv preprint arXiv:2410.03424*, 2024.

Haixu Wu, Jiehui Xu, Jianmin Wang, and Mingsheng Long. Autoformer: Decomposition transformers with auto-correlation for long-term series forecasting. *Advances in neural information processing systems*, 34:22419–22430, 2021.

Keyulu Xu, Weihua Hu, Jure Leskovec, and Stefanie Jegelka. How powerful are graph neural networks? *arXiv preprint arXiv:1810.00826*, 2018.

Tianzhu Ye, Li Dong, Yuqing Xia, Yutao Sun, Yi Zhu, Gao Huang, and Furu Wei. Differential transformer. In *The Thirteenth International Conference on Learning Representations*, 2025. URL https://openreview.net/forum?id=OvoCm1gGhN.

Guoqi Yu, Jing Zou, Xiaowei Hu, Angelica I Aviles-Rivero, Jing Qin, and Shujun Wang. Revitalizing multivariate time series forecasting: Learnable decomposition with inter-series dependencies and intra-series variations modeling. *arXiv preprint arXiv:2402.12694*, 2024.

Chulhee Yun, Srinadh Bhojanapalli, Ankit Singh Rawat, Sashank Reddi, and Sanjiv Kumar. Are transformers universal approximators of sequence-to-sequence functions? In *International Conference on Learning Representations*, 2020. URL https://openreview.net/forum?id=ByxRM0Ntvr.

Seongjun Yun, Minbyul Jeong, Raehyun Kim, Jaewoo Kang, and Hyunwoo J Kim. Graph transformer networks. *Advances in neural information processing systems*, 32, 2019.

Ailing Zeng, Muxi Chen, Lei Zhang, and Qiang Xu. Are transformers effective for time series forecasting? In *Proceedings of the AAAI conference on artificial intelligence*, volume 37, pp. 11121–11128, 2023.

Yunhao Zhang and Junchi Yan. Crossformer: Transformer utilizing cross-dimension dependency for multivariate time series forecasting. In *The Eleventh International Conference on Learning Representations*, 2023. URL https://openreview.net/forum?id=vSVLM2j9eie.

Lifan Zhao and Yanyan Shen. Rethinking channel dependence for multivariate time series forecasting: Learning from leading indicators. *arXiv preprint arXiv:2401.17548*, 2024.

A Implementation Details

A.1 Dataset Information

We provide additional information on the real-world datasets used in our experiments. ECL, ETT (4 variations), Traffic, and Weather datasets are from (Wu et al., 2021). Solar dataset is from (Lai et al., 2018). We use dataset information and descriptions from (Liu et al., 2024; Wang et al., 2024c; Zhang & Yan, 2023).

1. **ETTh1 & ETTh2** contain 7 indicators of an electricity transformer in two years, including oil temperature, load characteristics, etc. Data points are recorded every hour.
2. **ETTm1 & ETTm2** contain the same data as with the ETTh datasets but recorded over 15 minute intervals.
3. **Exchange** contains daily exchange rates data from 8 countries between 1990 and 2016.
4. **Weather** contains 21 meteorological indicators in the U.S over the entire year of 2020, including features like visibility, wind speed, etc.
5. **Solar** records solar power production of 137 PV plants in 2006, sampled every 10 minutes.

6. **ECL** records the hourly electricity consumption data of 321 clients.

7. **Traffic** records road occupancy rates measured by 862 sensors in San Francisco freeways from 2015 to 2016.

8. **PEMS (03, 08)** contain traffic flow data in California at 5 minutes intervals.

Table 3: Details of the datasets used in our experiments. The ETT datasets used training, validation, and testing split of 6:2:2 while the rest of the datasets used a 7:1:2 splits, in line with the experimental setups from (Liu et al., 2024; Zhang & Yan, 2023) and other baselines.

Dataset	**Dim**	**Prediction Length**	**Dataset Size**	**Frequency**	**Information**
ETTh1	7	{96, 192, 336, 720}	(8545, 2881, 2881)	Hourly	Electricity
ETTh2	7	{96, 192, 336, 720}	(8545, 2881, 2881)	Hourly	Electricity
ETTm1	7	{96, 192, 336, 720}	(34465, 11521, 11521)	15min	Electricity
ETTm2	7	{96, 192, 336, 720}	(34465, 11521, 11521)	15min	Electricity
Exchange	8	{96, 192, 336, 720}	(5120, 665, 1422)	Daily	Economy
Weather	21	{96, 192, 336, 720}	(36792, 5271, 10540)	10min	Weather
ECL	321	{96, 192, 336, 720}	(18317, 2633, 5261)	Hourly	Electricity
Traffic	862	{96, 192, 336, 720}	(12185, 1757, 3509)	Hourly	Transportation
Solar-Energy	137	{96, 192, 336, 720}	(36601, 5161, 10417)	10min	Energy
PEMS03	358	{12, 24, 48, 96}	(15617, 5135, 5135)	5min	Transportation
PEMS08	170	{12, 24, 48, 96}	(10690, 3548, 3548)	5min	Transportation

A.2 Experimental Details

All experiments are implemented in PyTorch (Paszke et al., 2019) and run on a single NVIDIA A100 80GB GPU. We use the ADAM (Kingma & Ba, 2014) optimizer and MSE loss function for all training. For more information on dataset-specific model configuration, refer to Table 4. For fair comparison against other transformer models, we follow the practices of recent state-of-the-art transformer baselines (Liu et al., 2024; 2025b; Zhang & Yan, 2023) and prepare our data with simple pre-processing steps and prediction block. Concretely, this means that we only use a linear layer for tokenization and do not make any use of more complicated signal processing techniques or data enriching strategies to enhance the model beyond its core technical contribution. For prediction, this also means that we are only using a linear layer as decoder for forecasting. One notable exception is reverse instance normalization, a widely adopted technique that is utilized in nearly every modern MTS architecture and is discussed further in Appendix A.4. These steps are taken strictly for benchmarking purposes and more sophisticated data engineering and forecasting methodologies should be integrated as seen fit in practical applications.

A.3 Metrics Used

For metrics used in our benchmarking, we utilize both mean squared error (MSE) and mean absolute error (MAE). MSE penalizes larger errors more heavily due to its quadratic nature, making it particularly sensitive to outliers. This characteristic is valuable for applications where large deviations are especially problematic. Conversely, MAE treats all error magnitudes linearly, providing a more robust measure of average model performance that is less influenced by occasional extreme predictions. By reporting both metrics, we offer a more comprehensive evaluation of model performance: MSE highlights models that avoid significant errors, while MAE better reflects the typical prediction accuracy a user might expect in practice.

Table 4: Model configurations across different datasets with iTransformer (Liu et al., 2024) backbone. We keep the hyperparameters used with standard attention (with dropout being the only exception) in prime attention to ensure fair comparison.

Dataset	**Model Hyper-Parameter**				**Training Process**		
	Model Dim	**Layers**	**Dropout**	**Learning Rate**	**Loss**	**Batch Size**	**Epochs**
ETTh1	256	2	0.1	0.0001	MSE	128	10
ETTh2	128	2	0.1	0.0001	MSE	128	10
ETTm1	128	2	0.2	0.0001	MSE	128	10
ETTm2	128	2	0.8	0.0001	MSE	128	10
Weather	128	3	0.4	0.0005	MSE	128	10
Electricity (ECL)	512	3	0.2	0.0005	MSE	4	10
Solar	128	6	0.2	0.0001	MSE	4	10
Traffic	128	4	0.2	0.001	MSE	2	10
Exchange	64	2	0.8	0.0001	MSE	128	10
PEMS03	512	4	0.1	0.0001	MSE	2	10
PEMS08	512	2	0.1	0.0001	MSE	4	10

$$MSE(y, \hat{y}) = \frac{1}{n}\sum_{i=1}^{n}(y_i - \hat{y}i)^2 \tag{21}$$

$$MAE(y, \hat{y}) = \frac{1}{n}\sum_{i=1}^{n}|y_i - \hat{y}_i| \tag{22}$$

A.4 Data Non-stationarity

MTS data exhibits pronounced non-stationarity characterized by persistent alterations in statistical attributes and joint distributions across time Liu et al. (2022). To tackle this issue, reverse instance normalization (RevIN) Kim et al. (2022) has been widely used in recent works, including all of the baseline transformers we are using to benchmark our proposed method. RevIN addresses distribution shift in MTS data by first normalizing input data using instance-specific statistics and then de-normalizing the model output to restore the original distribution. More formally,

$$\text{Normalization:} \quad \hat{x} = \gamma \cdot \frac{x - \mu_x}{\sigma_x} + \beta \tag{23}$$

$$\text{Denormalization:} \quad \hat{y} = \sigma_x \cdot \tilde{y} + \mu_x \tag{24}$$

where μ_x and σ_x are the instance-specific mean and standard deviation, while γ and β are learnable parameters.

RevIN makes up one of the most widely used pre-processing techniques in transformers for MTS forecasting. For the most part, however, recent MTS transformer keep pre-processing and data engineering simple and straight-forward to ensure fair and consistent comparisons against other works for benchmarking purposes. We also follow this paradigm in our experiments.

B Channel Strategies in MTS

Channel strategies in MTS are broadly divided into two categories: channel-independent (CI) (Zeng et al., 2023; Nie et al., 2022; Chen et al., 2025) and channel-dependent (CD) (Liu et al., 2024; Wang et al., 2024b;a). CI approaches model each channel independently without any cross-channel interactions, which bypasses the channel heterogeneity problem entirely. CI approaches have been shown to be highly robust but crucially lack capacity (Han et al., 2024) and generalizability (Qiu et al., 2025).

CD approaches, on the other hand, argue that certain patterns crucial for accurate MTS forecasting such as lagged information (Liu et al., 2025a; Zhao & Shen, 2024) or intricate correlations and physical laws (Chen et al., 2023; Yu et al., 2024) can only be captured by inter-channel modeling. Therefore, CD approaches allow cross-channel interactions to capture inter-channel relationships crucial for accurate forecasting. As a result, CD methods are susceptible to the potentially complex and heterogeneous inter-channel dynamics that, if not captured correctly, can lead to noise accumulation and performance degradation. Our proposed prime attention is a CD approach that explicitly tackles the channel-heterogeneity problem for transformers in MTS with the aim of making channel-wise attention more favorable in the domain of time series.

C Limitations and Future Work

Despite consistent improvements across the board in Section 7 and some interesting properties such as those shown in the sequence length and memory analyses in Appendices G.2 and G.4, there are limitations of prime attention worth considering. First, it is unclear how much benefit prime attention brings to systems with homogeneous information such as Traffic and ECL. As mentioned in Section 7, prime attention only outperforms standard attention marginally in such cases. In addition, the memory requirements of prime attention can be quite high and while we provide a sparsification strategy in Appendix D.2, prime attention's marginal improvements on certain systems may still favor standard attention in such cases. An interesting future work could entail exploring sparsification approaches that are more sophisticated in determining which channel-pairs get pair-wise modulation and which channel-pairs do not. For example, one could create a hybrid attention mechanism where homogeneous channel-pairs are processed with standard attention and heterogeneous channel-pairs get prime attention. This could be understood via graph rewiring approaches with two distinct graph topologies: one for standard attention and the other for prime attention. The GNN framework for prime attention discussed in Appendix D.2 could serve as the backbone for this approach. Overall, we believe that future work could benefit from enabling prime attention in a more diverse array of systems and improving its practicality with strategies such as sophisticated sparsification or hybrid attention.

D Prime Attention for Graph Neural Networks

D.1 Graph Neural Networks Background

In this section, we provide the necessary background for machine learning on graph data, or graph neural networks (GNNs). Much of the information presented here is derived from (Hamilton, 2020).

A graph $\mathcal{G} = (V, E)$ consists of a set of nodes (also called vertices) $V = \{v_1, v_2, \ldots, v_N\}$ and edges (also called links) $E \subseteq V \times V$ that define connections between nodes. Each node v_i is associated with a feature vector $h_i \in \mathbb{R}^d$, and edges may optionally carry features $e_{ij} \in \mathbb{R}^{d_e}$. The neighborhood of node v_i is denoted as $\mathcal{N}(i) = \{j : (v_i, v_j) \in E\}$. Graphs provide a natural way to model relational data where entities (nodes) have features and relationships (edges) define interactions. This structure is ubiquitous in domains ranging from social networks and molecular chemistry to knowledge graphs and MTS where channels exhibit dependency relationships.

Message Passing Framework GNNs operate on the message passing paradigm, which consists of the aggregate and update functions. A message passing step for a single node v_i can be expressed as:

$$h_i^{(t+1)} = UPDATE^{(t)}(h_i^{(t)}, AGGREGATE^{(t)}(\{h_j^{(t)}, \forall j \in \mathcal{N}(i)\})) \tag{25}$$

where $AGGREGATE$ combines the node representations (and optionally edge information) of the neighborhood of node i and $UPDATE$ uses the aggregated neighborhood information along with representation for node i at the current layer to update its representation for the next layer. The choice of $AGGREGATE$ and its effect on performance has been studied extensively in the literature and common choices include sum, mean, max, or attention-weighted combinations. The $UPDATE$ function, which determines how nodes evolve their internal representations by integrating neighborhood information with their current representation, is typically an MLP.

Graph Convolutional Network Graph Convolutional Networks (GCN) implement a simple message passing scheme using summation with symmetric normalization for aggregation and an MLP for update:

$$h_i^{(t+1)} = \sigma(W^{(t)} \sum_{j \in \mathcal{N}(i) \cup \{i\}} \frac{h_j^{(t)}}{\sqrt{|\mathcal{N}(i)||\mathcal{N}(j)|}}) \tag{26}$$

where σ is a non-linear activation function and W is the learnable weight matrix. The symmetric normalization of GCN ensures stable message propagation across nodes with different degrees.

Graph Attention Networks Graph Attention Networks (GAT) extend the graph neural network paradigm by introducing an attention mechanism that allows each node to dynamically weight the importance of its neighbors during message passing. For a given node , GAT computes attention coefficients for each neighbor based on a shared learnable function that considers both nodes' feature embeddings. Mathematically, these coefficients are calculated by applying a nonlinear transformation and softmax normalization to the concatenated features, typically as:

$$\text{GAT (Veličković et al., 2017)} \quad \alpha_{ij} = softmax(LeakyReLU(a^T \cdot [Wh_i||Wh_j])) \tag{27}$$

$$\text{GATv2 (Brody et al., 2021)} \quad \alpha_{ij} = softmax(a^T LeakyReLU(W \cdot [h_i||h_j])) \tag{28}$$

where a is a learned attention vector. GATv2 improves upon GAT by de-coupling the linear combination of a with $Wh_i||Wh_j$ and instead making it a non-linear combination. The node update then becomes:

$$h_i = \sigma(\sum_{j \in \mathcal{N}(i) \cup \{i\}} \alpha_{ij} Wh_j) \tag{29}$$

where σ is an activation function and neighborhood representations are aggregated in a weighted sum according to the comptued attention weights. GAT can be seen as a sparse and localized variant of standard attention in transformers. Thus, much like transformer's success in the language domain, GAT has been widely adopted and shown to be performant across the graph domain.

Graph Isomorphism Networks Graph Isomorphism Network (GIN) represent a theoretically principled approach to maximizing the expressive power of graph neural networks by aligning their computational framework with the Weisfeiler-Leman (WL) graph isomorphism test. The key insight behind GIN is that standard GNN aggregation functions (mean, max-pooling) may fail to distinguish certain graph structures due to their inability to capture multiset cardinalities—different collections of neighbor features that yield identical aggregated representations. GIN addresses this limitation through an injective aggregation function that preserves distinctness of multisets:

$$h_i^{(t+1)} = MLP((1 + \epsilon^{(t)}) \cdot h_i^{(t)} + \sum_{j \ in \mathcal{N}(i)} h_j^{(t)}) \tag{30}$$

where $\epsilon^{(t)}$ is either a learnable parameter or fixed constant, and the summation ensures injectivity by preserving multiset structure.

D.2 Adapting Prime Attention to Graphs

Graph Neural Networks (GNNs) (Hamilton et al., 2017; Xu et al., 2018; Gilmer et al., 2017) provide a natural framework for modeling structured relationships in data by restricting computations to meaningful connections defined by graph topology (see Appendix D.1 for background information on GNNs). We show how prime attention can be adapted for Graph Attention Networks (GATs) (Veličković et al., 2017; Brody et al., 2021), which are a class of GNNs that use attention mechanism for relational learning. This adaptation of prime attention provides considerable resource efficiency over full attention while maintaining topologically relevant connections.

Standard GAT operating on graph $\mathcal{G}$ restricts attention computation to graph neighborhoods defined by the adjacency matrix $\mathcal{A}$, where for node i, only its neighbors $j \in \mathcal{N}_i$ are considered for pair-wise modeling. For our context, assume $\mathcal{A}$ to be binary and the graph to be undirected. Unlike other GNNs of its class (Kipf, 2016; Xu et al., 2018; Gilmer et al., 2017), a GAT layer is capable of performing relational learning (albeit static) by performing weighted sums of each node's neighborhood information based on learned relationship importance.

The connectivity of the graph, defined by $\mathcal{A}$, can be informed by underlying topological context (such as road network being represented as a graph in traffic data) or constructed purely as a computational graph. Expander graphs designed for GNNs (Deac et al., 2022; Wilson et al., 2024) are a class of computational graphs with mathematical properties that simultaneously guarantee high connectivity and sparsity of connections and are therefore a suitable choice for data with no underlying graph topology. With an appropriate $\mathcal{G}$, standard GAT computation formulated by (Veličković et al., 2017) is:

$$h_i' = \sigma\left(\sum_{j\in\mathcal{N}_i} softmax_j\left(e(h_i, h_j)\right) W h_j\right) \tag{31}$$

and $e(\cdot)$ is an attention scoring function defined in (Brody et al., 2021) as:

$$e(h_i, h_j) = a^T LeakyReLU(W \cdot [h_i || h_j]) \tag{32}$$

where $\sigma(\cdot)$ is an element-wise nonlinearity, $h_i, h_j \in \mathbb{R}^{d_{model}}$ denote node (or channel) representations, $W \in \mathbb{R}^{d_{model}\times d_{model}}$ denotes the weight matrix, and $||$ denotes concatenation operation.

GAT with prime attention extends this setup by incorporating dynamic pair-specific modulation while maintaining the sparse structure:

$$\widetilde{h}_i' = \sigma\left(\sum_{j\in\mathcal{N}_i} softmax_j\left(e(h_i, \widetilde{h}_j)\right) W \widetilde{h}_j\right) \tag{33}$$

$$\widetilde{h}_j = h_j \odot \mathcal{F}_{i,j} \tag{34}$$

where the key difference here is that as opposed to full prime attention, the modulator $\mathcal{F}$ are only learned and applied for connected node pairs, reducing its memory footprint from $\mathcal{O}(N^2 \times d_{model})$ to $\mathcal{O}(|E| \times d_{model})$ where $|E|$ represents the number of edges in the graph and $|E| \ll N^2$. The overall attention complexity is also reduced to $\mathcal{O}(|E| \times d_{model})$.

Prime attention's adaptation to GNNs represents a natural pathway for achieving computational scalability while preserving topological context. By restricting pair-specific modulation to meaningful edges in a learned or predefined graph structure, we reduce both memory and computational requirements from the dense $O(N^2 \times d_{model})$ to sparse $O(|E| \times d_{model})$ complexity. This graph-based formulation can also be useful in MTS applications where physical relationships, causal dependencies, or correlation structures can inform useful relational topologies—for instance, spatial proximity in sensor networks.

E Universal Approximation Theorem for Prime Attention

Standard attention mechanism in transformers have been proven to satisfy the universal approximation theorem. Given sufficient depth, width, and training data, standard attention can approximate any continuous sequence-to-sequence function to arbitrary precision (Cybenko, 1989; Yun et al., 2020). By showing that prime attention contains standard attention, we make a simple theoretical claim that prime attention also satisfies the universal approximation theorem and its guarantees.

Theorem E.1. *Prime attention satisfies the universal approximation theorem.*

Proof. We examine the function class relationship between prime attention and standard attention. Let $\mathcal{H}_{\text{standard}}$ denote the function class representable by standard attention and $\mathcal{H}_{\text{prime}}$ denote the function class representable by prime attention. Prime attention extends standard attention by introducing learnable element-wise modulation filters $\mathcal{F}_{ij} \in \mathbb{R}^{d\text{model}}$ for each token pair (x_i, x_j):

$$\widetilde{k}_j^{(i)} = k_j \odot \mathcal{F}_{ij}, \quad \widetilde{v}_j^{(i)} = v_j \odot \mathcal{F}_{ij} \tag{35}$$

We make the observation that prime attention strictly contains standard attention as a special case in its function class. Notably, when setting all modulation filters to the identity $\mathcal{F}_{ij} = 1_{d_{model}}$, $\forall i, j \in \{1, ..., N\}$, prime attention is reduced to:

$$\widetilde{k}_j^{(i)} = k_j \odot 1_{d_{model}} = k_j, \quad \widetilde{v}_j^{(i)} = v_j \odot 1_{d_{model}} = v_j \tag{36}$$

which equates to standard attention. Since $\mathcal{F}_{ij} \in \mathbb{R}^{d_{model}}$ and $1_{d_{model}} \subset \mathbb{R}^{d_{model}}$, we can show $\mathcal{H}_{\text{standard}} \subseteq \mathcal{H}_{\text{prime}}$. Therefore, prime attention can approximate *at least* all functions that standard attention can approximate. Since standard attention satisfies the universal approximation guarantees and can approximate any continuous sequence-to-sequence function $f : \mathbb{R}^{n\times d} \to \mathbb{R}^{m\times d}$ to arbitrary precision given sufficient resources, and since $\mathcal{H}_{\text{standard}} \subseteq \mathcal{H}_{\text{prime}}$, prime attention inherits the universal approximation guarantees of standard attention.

This theoretical guarantee ensures that prime attention does not sacrifice any representational capabilities of standard attention and that any function learnable by standard attention is also learnable by prime attention. As with standard attention's universal approximation guarantees, this assumes sufficient model depth and width as well as adequate training data and appropriate optimization strategy. In addition, proper initialization and training of learnable modulator $\mathcal{F}$ is also crucial.

F Gradient Flow Analysis for Prime Attention

We provide a gradient flow analysis comparing standard attention and prime attention. This analysis assumes a single layer with one attention head.

For both mechanisms, assume the input data $X \in \mathbb{R}^{N\times d_{model}}$ where N is the number of tokens and d_{model} is the model dimension. For standard attention,

$$Q = XW_Q, \quad K = XW_K, \quad V = XW_V \tag{37}$$

where $W_Q, W_K, W_V \in \mathbb{R}^{d_{model}\times d_{model}}$ are projection matrices.

Standard Attention Gradient Flow The forward computation flow for standard attention is:

$$A = softmax(\frac{QK^T}{\sqrt{d_{model}}}) \tag{38}$$

$$O = AV \tag{39}$$

Given the gradient of O as $\frac{\partial L}{\partial O}$ for standard attention, the gradients of parameters are formulated via:

$$\frac{\partial L}{W_V} = \frac{\partial L}{\partial O}\frac{\partial O}{\partial V}\frac{\partial V}{\partial W_V} \tag{40}$$

$$= X^T A^T (\frac{\partial L}{\partial O}) \tag{41}$$

$$\frac{\partial L}{\partial W_Q} = \frac{\partial L}{\partial O}\frac{\partial O}{\partial A}\frac{\partial A}{\partial Q}\frac{\partial Q}{\partial W_Q} \tag{42}$$

$$= \frac{1}{\sqrt{d_{model}}} X^T [A \odot (\frac{\partial L}{\partial O} V^T - A \odot (\frac{\partial L}{\partial O} V^T)J)]K \tag{43}$$

$$\frac{\partial L}{\partial W_K} = \frac{\partial L}{\partial O}\frac{\partial O}{\partial A}\frac{\partial A}{\partial K}\frac{\partial K}{\partial W_K} \tag{44}$$

$$= \frac{1}{\sqrt{d_{model}}} X^T [A \odot (\frac{\partial L}{\partial O} V^T - A \odot (\frac{\partial L}{\partial O} V^T)J)]Q \tag{45}$$

Prime Attention Gradient Flow Prime attention extends standard attention's computation with learnable pair-wise modulators that are applied to K and V as:

$$\widetilde{K} = K \odot \mathcal{F}, \quad \widetilde{V} = V \odot \mathcal{F} \tag{46}$$

where we assume the full modulator $\mathcal{F} \in \mathbb{R}^{N \times N \times d_{model}}$. Then, the forward flow for prime attention is:

$$\widetilde{A} = softmax(\frac{Q\widetilde{K}^T}{\sqrt{d_{model}}}) \tag{47}$$

$$\widetilde{O} = \widetilde{A}\widetilde{V} \tag{48}$$

Given the gradient of $\widetilde{O}$ as $\frac{\partial L}{\partial \widetilde{O}}$ for prime attention, the gradients of parameters are formulated via:

$$\frac{\partial L}{\partial W_V} = \frac{\partial L}{\partial \widetilde{O}}\frac{\partial \widetilde{O}}{\partial \widetilde{V}}\frac{\partial \widetilde{V}}{\partial V}\frac{\partial V}{\partial W_V} \tag{49}$$

$$= X^T (\widetilde{A}^T \odot \mathcal{F}^T)\frac{\partial L}{\partial \widetilde{O}} \tag{50}$$

$$\frac{\partial L}{\partial W_Q} = \frac{\partial L}{\partial \widetilde{O}}\frac{\partial \widetilde{O}}{\partial \widetilde{A}}\frac{\partial \widetilde{A}}{\partial Q}\frac{\partial Q}{\partial W_Q} \tag{51}$$

$$= (\frac{1}{\sqrt{d_{model}}}) X^T [\widetilde{A} \odot (\frac{\partial L}{\partial \widetilde{O}} \widetilde{V}^T - (\widetilde{A}^T \odot (\frac{\partial L}{\partial \widetilde{O}} \widetilde{V}^T))J)]\widetilde{K} \tag{52}$$

$$\frac{\partial L}{\partial W_K} = \frac{\partial L}{\partial \widetilde{O}}\frac{\partial \widetilde{O}}{\partial \widetilde{A}}\frac{\partial \widetilde{A}}{\partial \widetilde{K}}\frac{\partial \widetilde{K}}{\partial K}\frac{\partial K}{\partial W_K} \tag{53}$$

$$= (\frac{1}{\sqrt{d_{model}}}) X^T ([\widetilde{A} \odot (\frac{\partial L}{\partial \widetilde{O}} \widetilde{V}^T - (\widetilde{A}^T \odot (\frac{\partial L}{\partial \widetilde{O}} \widetilde{V}^T))J)]^T \odot \mathcal{F}^T)Q \tag{54}$$

and the gradient with respect to $\mathcal{F}$ across multiple paths is formulated as:

$$\frac{\partial L}{\partial \mathcal{F}_{\text{path1}}} = \frac{\partial L}{\partial \widetilde{O}} \frac{\partial \widetilde{O}}{\partial \widetilde{A}} \frac{\partial \widetilde{A}}{\partial \widetilde{K}} \frac{\partial \widetilde{K}}{\partial \mathcal{F}} \tag{55}$$

$$= (\frac{1}{\sqrt{d_{model}}}) K \odot [Q^T(\widetilde{A}^T \odot [\frac{\partial L}{\partial \widetilde{O}} \widetilde{V}^T - (\widetilde{A}^T \odot (\frac{\partial L}{\partial \widetilde{O}} \widetilde{V}^T))J])] \tag{56}$$

$$\frac{\partial L}{\partial \mathcal{F}_{\text{path2}}} = \frac{\partial L}{\partial \widetilde{O}} \frac{\partial \widetilde{O}}{\partial \widetilde{V}} \frac{\partial \widetilde{V}}{\partial \mathcal{F}} \tag{57}$$

$$= V \odot [\widetilde{A}^T \frac{\partial L}{\partial \widetilde{O}}] \tag{58}$$

$$\frac{\partial L}{\partial \mathcal{F}} = \frac{\partial L}{\partial \mathcal{F}_{\text{path1}}} + \frac{\partial L}{\partial \mathcal{F}_{\text{path2}}} = \frac{\partial L}{\partial \widetilde{O}} \frac{\partial \widetilde{O}}{\partial \widetilde{A}} \frac{\partial \widetilde{A}}{\partial \widetilde{K}} \frac{\partial \widetilde{K}}{\partial \mathcal{F}} + \frac{\partial L}{\partial \widetilde{O}} \frac{\partial \widetilde{O}}{\partial \widetilde{V}} \frac{\partial \widetilde{V}}{\partial \mathcal{F}} \tag{59}$$

$$= (\frac{1}{\sqrt{d_{model}}}) K \odot [Q^T(\widetilde{A}^T \odot [\frac{\partial L}{\partial \widetilde{O}} \widetilde{V}^T - (\widetilde{A}^T \odot (\frac{\partial L}{\partial \widetilde{O}} \widetilde{V}^T))J])] + V \odot [\widetilde{A}^T \frac{\partial L}{\partial \widetilde{O}}] \tag{60}$$

This gradient flow analysis shows how prime attention introduces controlled parameters through the dynamic modulator $\mathcal{F}$, which creates additional gradient pathways for learning pair-wise relational information while maintaining similar overall gradient flow structure as standard attention.

G Additional Analysis and Experiments

G.1 Ablation Studies

Sparsity Ablation We conduct an ablation study on the effect of sparsifying the pair-wise primer $\mathcal{F}$ such that only a certain percentage of token pairs are modulated with $\mathcal{F}$ at random and the rest effectively perform standard attention. The results are shown in Figure 2 where sparsity on the x-axis refers to the percentage of token-pairs not getting a pair-wise modulator.

This analysis reveals a nuanced relationship between the degree of pair-wise modulation and model performance. We find that 100% sparsity (effectively standard attention) always performs significantly worse than having even 20% of token pairs be assigned a pair-wise primer. However, we do not necessarily see a positively correlated relationship between pair-wise priming and performance and note that having less sparsity (and therefore more pair-wise primers) does not always result in superior performance. In fact, on some datasets, having some degree of sparsity in $\mathcal{F}$ slightly improved performance. Considering the memory requirements of prime attention, and our observation here that any amount of pair-wise modulation improves upon standard attention, it may be useful in practice to take sparsity as a hyperparameter and optimize for the highest degree of sparsity that still results in acceptable performance gains.

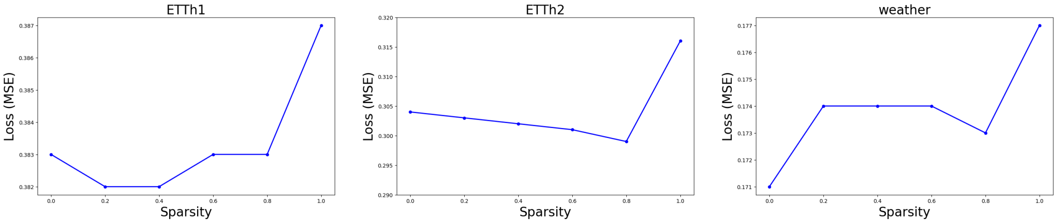

(a) (b) (c)

Figure 2: Ablation study on sparsity of pair-wise modulator $\mathcal{F}$. Sparsity refers to the amount (in percentage) of token pairs getting modulated (from left to right, 0% sparsity is full pair-wise modulation and 100% sparsity is equivalent to standard attention).

Filter Ablation We study the effects of different initialization strategies for $\mathcal{F}$. We look at four initialization strategies and chart each of their performance across increasing prediction horizons

$H \in \{96, 192, 336, 720\}$. Note that in all cases, the initialized modulator is made learnable with a 2-layer MLP. First, random initialization (in blue) uses Glorot initialization Glorot & Bengio (2010) centered around 1.0 to allow the model to effectively start at standard attention and learn relevant pair-wise relationships from scratch. We note that this generally performs worse than more sophisticated, domain appropriate strategies, as we show next. Second, we show initialization using estimated lead-lag information (in orange). This is mentioned in Section 5 and shows robust performance. Third, we initialize the modulator with instantaneous information and chart its performance in green. The estimated instantaneous correlation is calculated using a combination of Pearson correlation, rolling standard deviation, and rank-transformation information between channel pairs. We note that while this performs better than random initialization, it typically performs worse than lead-lag initialization. Lastly, we combine the lead-lag estimation and instantaneous correlations to create a full initialization (in red). The MLP takes both information and decides which information is more relevant for each channel-pair. Full initialization by far performs the best and shows stable performance and is used in our prime attention implementations.

Since these are merely initialization strategies, the MLP can ultimately learn to retain, modify, or even discard any information presented by more sophisticated initializations. Since MLPs satisfy the universal approximation theorem, given sufficient resources, the random initialization should be able to perform just as well as the full initialization across any given dataset. However, as discussed in Section 6, we find that injecting useful information to bias the model can make noticeable differences in practical scenarios.

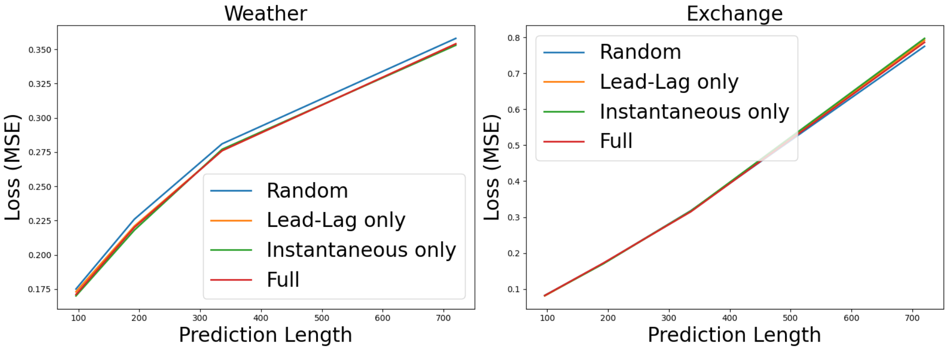

Figure 3: Effect that different initialization strategies for pair-wise modulation primer $\mathcal{F}$ has on performance (y-axis, lower is better) across prediction lengths (x-axis).

G.2 Complexity Analysis

We report empirical memory and time usage of prime attention using the Weather dataset and use standard attention as baseline. The results are shown in Figure 4. We use a Graph Attention Network (GAT) (Veličković et al., 2017; Brody et al., 2021) as the base architecture and systematically increase the density of the adjacency matrix to record memory and time usage for both standard and prime attention. The density of the adjacency matrix refers to how many pair-wise connections are allowed as a percentage of a fully connected graph. In other words, higher adjacency matrix density indicates more pair-wise channel interactions and 100% density essentially becomes regular full, quadratic attention. In each case, a random graph is constructed based on the prescribed density.

While Figure 4 shows that prime attention indeed uses more memory and computation time than standard attention, the discrepancy is not so straightforward when considering performance (forecasting accuracy). To illustrate this point, we denote with red stars the points of equivalent performance of standard and prime attention. As it can be seen, prime attention using 60% adjacency matrix density matches standard attention's performance at 100% density. At 60% density, prime attention uses less memory and computation time than standard attention at 100% density (their gaps are shown as green triangles). This shows that prime attention is capable of having lower *effective* complexity than standard attention since prime attention using less data, memory, and computation time can, in certain instances, match or outperform standard attention.

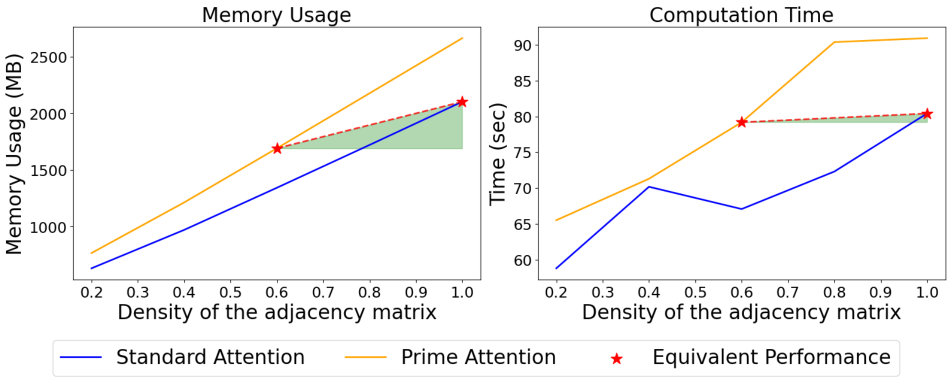

Figure 4: Analysis of memory (left) and computation time (right) for standard (blue) and prime (yellow) attention on the Weather dataset. The red star indicates observed equivalent performance (loss in MSE) between standard and prime attention.

G.3 Attention Map Analysis

We perform attention map analysis for standard attention, prime attention, and their difference map to show the change from standard attention map to prime attention map. As shown in Figure 5, prime attention's attention coefficient distribution has similarities to standard attention but also notable differences as seen in their difference map. The difference map is a good illustration of where standard and prime attention differ in their focus, with warmer colors (beige/red) indicating stronger focus from prime attention and colder colors (blue) indicating weaker focus from prime attention with respect to standard attention.

The attention maps of Solar dataset in Figure 6 demonstrates an interesting property of prime attention. As it can be seen, the standard attention map on the left shows disproportionate focus on one particular variable (shown as a thin yellow vertical line on the middle-right). While this is certainly not a problem in isolation, the fact that all channels have an over-reliance on a single particular channel while not valuing its own signals at all (along the diagonal) can potentially indicate that the model is collapsing to an easy solution and not necessarily a good one. In addition, an over-reliance on a single (or a small number of) signal(s) can be problematic as it can present a single point of failure in deployed systems whereby a loss of one sensor can devastate the performance of the entire system. Prime attention, on the other hand, completely remedies this issue and illustrates how the benefits of pair-wise modulation includes self-attention. Instead of putting an over-reliance on a single channel, prime attention enables effective pattern discovery for self-attention and learns to take the form of a *soft* CI model, whereby the model essentially learns to be channel-independent (given limitations of softmax). It's performance improvement of 3.8% from standard attention verifies the validity of this approach on this particular dataset.

In contrast to its ability to learn to be a soft CI model, Figure 7 demonstrates an instance where prime attention learns to do the opposite by learning to weaken its self-attention instead. As it can be seen from the difference map, prime attention actually weakens the contribution of self-attention of many channels in Figure 7, and instead strengthens a selection of cross-channel interactions.

Overall, attention map analysis for standard and prime attention on various datasets show that prime attention's relational modeling may be potent enough to act as a hybrid CD/CI model. While this is not the main focus of this work, it may merit further analysis for future work.

G.4 Sequence Length Analysis

Here, we perform a sequence length (or look-back window length L) analysis for standard and prime attention. Namely, we are interested in seeing how performance improves with longer sequence length (or more input data). Performance for each model is measured across $L \in \{16, 32, 48, 64, 80, 96\}$ and the prediction horizon is fixed at $H = 96$. We show the results in Figure 1.

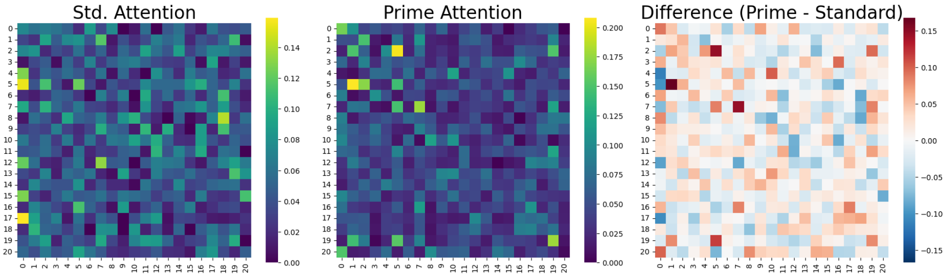

Figure 5: Attention maps of standard attention (left), prime attention (middle), and their difference (right) on the Weather dataset. Warmer colors (yellow/green) reflect higher attention coefficient and colder colors (blue/purple) reflect lower attention coefficient.

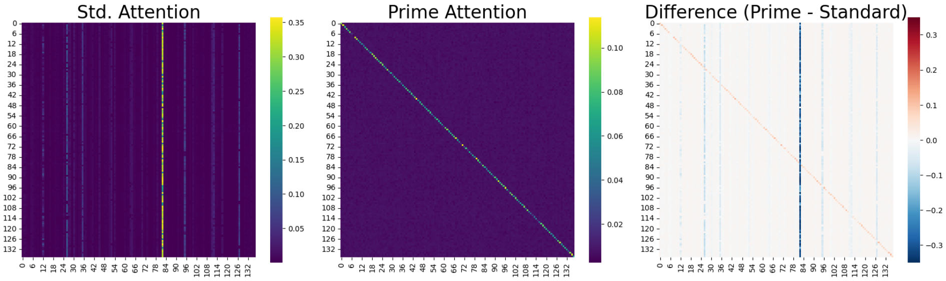

Figure 6: Attention maps of standard attention (left), prime attention (middle), and their difference (right) on the Solar dataset. Warmer colors (yellow/green) reflect higher attention coefficient and colder colors (blue/purple) reflect lower attention coefficient.

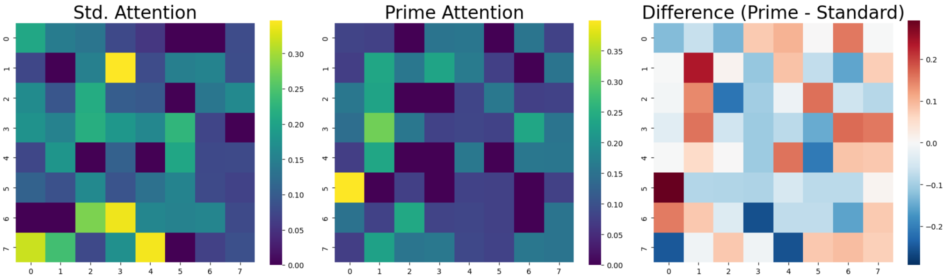

Figure 7: Attention maps of standard attention (left), prime attention (middle), and their difference (right) on the Exchange dataset. Warmer colors (yellow/green) reflect higher attention coefficient and colder colors (blue/purple) reflect lower attention coefficient.

Remarkably, prime attention not only shows improved performance at each L as expected, but it also shows that it can match or slightly outperform standard attention's performance with significantly less input sequence length in some instances. To illustrate this, we use a horizontal green dotted line labeled *target threshold* to mark the performance of standard attention when using $L = 96$. As shown in Figures 1a and 1b, prime attention breaks through the target threshold using sequence lengths of 48 and 64, which translates to using 40% and 33% less input data compared to standard attention, respectively. While such significant results were not observed across all datasets, it does align well with the observed benefits of inductive biases in other domains. It also strengthens our argument in Section 6 that prime attention acts as a learnable inductive bias in attention to enable and accelerate effective discoveries of unique relational dynamics across pair-wise interactions. In addition, this finding may be of interest in domains where input data is scarce.

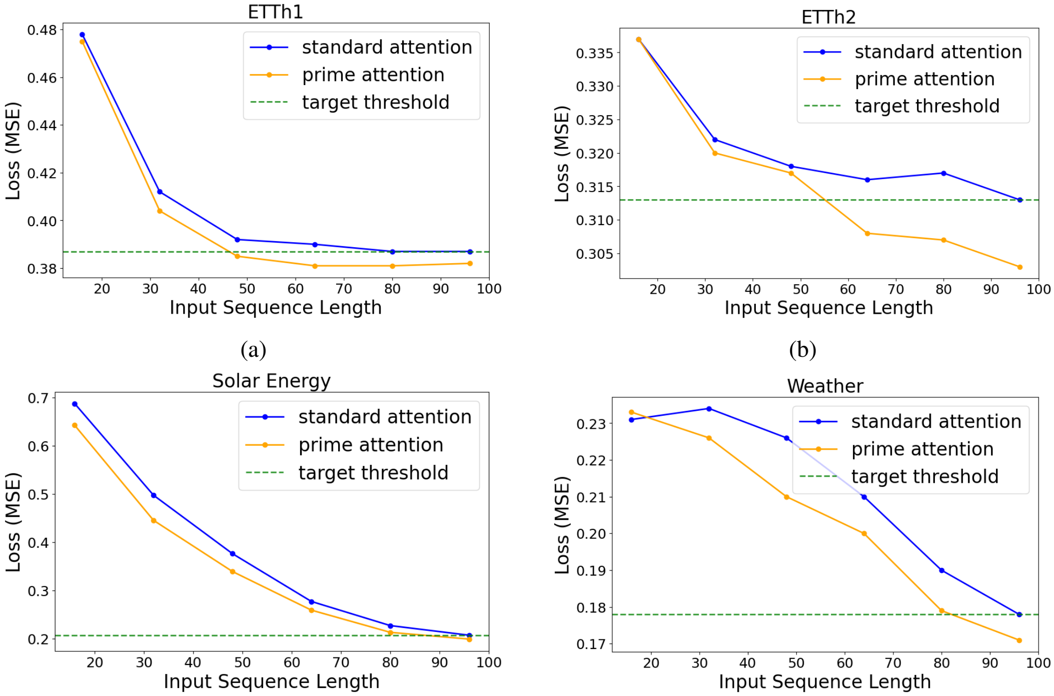

(a)

(b)

(c)

(d)

Figure 8: Comparing performance between standard (blue) and prime (yellow) attention at various input sequence length (or look-back window L). The horizontal target threshold line (green, dotted) represents standard attention's performance at $L = 96$.

H Full Forecasting Results

Unless otherwise stated, forecasting experiments have the look-back window L set to 96 and predictions are made on horizons $H \in \{96, 192, 336, 720\}$ except on the PEMS data, where $H \in \{12, 24, 48, 96\}$. Avg. indicates the averaged loss value of all horizons.

We provide the full comparison between prime attention and existing works in MTS that enhance and leverage relation information in Table 5. The best performance from each row is denoted in **bold**.

We provide the full forecasting results in Table 6. Each model's original baseline performance using standard attention is displayed side-by-side with its updated performance using prime attention. Standard attention refers to the baseline full-attention (or its equivalent) that the transformer model was originally equipped with. To test prime attention's impact on overall transformer model performance, the transformer is first fine-tuned on standard attention and its attention module is subsequently replaced with prime attention only adjusting dropout rate. The better performance (between standard and prime attention) within each model is shown in **teal** when prime attention is better and in **brown** when standard attention is better. Overall, using prime attention outperforms the original baselines consistently across all datasets and models, with up to 6.5% improvement in performance for the Weather dataset.

Table 5: Performance comparison between prime attention and existing works in MTS that enhance and leverage relational information. Prime attention is using iTransformer Liu et al. (2024) as backbone.

	Model	***Prime Attn.* (Ours)**		DIFF Transformer (2025)		LagTS (2025)		LIFT (2024)		Autoformer (2021)	
	Metrics	MSE	MAE	MSE	MAE	MSE	MAE	MSE	MAE	MSE	MAE
ETTh1	96	**0.379**	**0.398**	0.385	0.400	0.384	0.402	0.385	0.404	0.449	0.459
	192	0.432	**0.428**	0.438	0.431	0.437	0.435	**0.431**	0.429	0.500	0.482
	336	0.472	0.449	0.480	0.453	**0.470**	**0.449**	0.475	0.450	0.521	0.496
	720	0.478	0.475	0.479	0.477	**0.466**	**0.469**	0.479	0.473	0.514	0.512
	Avg.	0.440	**0.438**	0.446	0.440	**0.439**	0.439	0.443	0.439	0.496	0.487
ETTh2	96	**0.296**	**0.348**	0.309	0.360	0.305	0.351	0.306	0.351	0.346	0.388
	192	**0.374**	0.399	0.385	0.405	0.381	**0.399**	0.390	0.406	0.456	0.452
	336	0.416	0.428	0.422	0.434	**0.416**	**0.428**	0.418	0.429	0.482	0.486
	720	**0.420**	**0.441**	0.428	0.446	0.425	0.444	0.427	0.446	0.515	0.511
	Avg.	**0.377**	**0.404**	0.386	0.411	0.382	0.405	0.386	0.408	0.450	0.459
Exchange	96	0.083	0.201	**0.083**	**0.201**	0.085	0.206	0.085	0.205	0.197	0.323
	192	**0.172**	0.295	0.173	**0.295**	0.181	0.304	0.178	0.302	0.300	0.369
	336	**0.314**	**0.405**	0.332	0.418	0.331	0.416	0.328	0.415	0.509	0.524
	720	0.786	0.668	0.839	0.690	**0.768**	**0.663**	0.831	0.691	1.447	0.941
	Avg.	**0.339**	**0.392**	0.357	0.401	0.341	0.397	0.356	0.403	0.613	0.539
Weather	96	**0.170**	**0.210**	0.176	0.215	0.173	0.216	0.172	0.216	0.266	0.336
	192	**0.218**	**0.254**	0.225	0.258	0.224	0.260	0.225	0.260	0.307	0.367
	336	**0.276**	**0.296**	0.280	0.299	0.280	0.300	0.283	0.302	0.359	0.395
	720	**0.351**	**0.347**	0.356	0.349	0.355	0.349	0.358	0.350	0.419	0.428
	Avg.	**0.254**	**0.277**	0.259	0.280	0.258	0.281	0.260	0.282	0.338	0.382

Table 6: Comparison between standard attention and prime attention on recent state-of-the-art transformer models.

Model		Timer-XL (2025)				FreDF (2025)				iTransformer (2024)			
Attn Type		Standard		***Prime***		Standard		***Prime***		Standard		***Prime***	
		MSE	MAE	MSE	MAE	MSE	MAE	MSE	MAE	MSE	MAE	MSE	MAE
ETTh1	96	0.380	0.398	**0.377**	**0.394**	0.380	0.394	**0.376**	**0.392**	0.387	0.403	**0.379**	**0.398**
	192	0.432	0.429	**0.428**	**0.424**	0.434	0.426	**0.430**	**0.423**	0.439	0.432	**0.432**	**0.428**
	336	0.473	0.453	**0.469**	**0.448**	0.479	0.451	**0.473**	**0.448**	0.482	0.455	**0.472**	**0.449**
	720	0.528	0.500	**0.478**	**0.473**	**0.516**	**0.500**	0.517	0.501	0.489	0.481	**0.478**	**0.475**
	Avg.	0.453	0.445	**0.438**	**0.435**	0.452	0.443	**0.449**	**0.441**	0.449	0.443	**0.440**	**0.438**
ETTh2	96	0.298	0.348	**0.293**	**0.345**	0.289	0.340	**0.286**	**0.337**	0.315	0.361	**0.296**	**0.348**
	192	0.383	0.402	**0.376**	**0.398**	0.382	0.400	**0.380**	**0.395**	0.380	0.402	**0.374**	**0.399**
	336	0.435	0.441	**0.429**	**0.438**	**0.438**	0.444	0.438	**0.443**	0.421	0.431	**0.416**	**0.428**
	720	0.467	0.469	**0.458**	**0.465**	0.451	**0.461**	**0.450**	0.460	0.423	0.443	**0.420**	**0.441**
	Avg.	0.396	0.415	**0.389**	**0.412**	0.390	0.411	**0.389**	**0.409**	0.385	0.409	**0.377**	**0.404**
ETTm1	96	0.329	0.364	**0.321**	**0.359**	0.325	0.359	**0.318**	**0.353**	0.337	0.371	**0.325**	**0.363**
	192	0.394	0.403	**0.384**	**0.397**	0.374	0.384	**0.368**	**0.382**	0.377	0.392	**0.368**	**0.388**
	336	0.458	0.441	**0.444**	**0.433**	0.418	0.411	**0.415**	**0.409**	0.420	0.418	**0.405**	**0.412**
	720	0.581	0.503	**0.560**	**0.491**	**0.492**	**0.454**	0.500	0.462	0.487	0.456	**0.476**	**0.451**
	Avg.	0.441	0.428	**0.427**	**0.420**	0.402	**0.402**	**0.400**	0.402	0.405	0.409	**0.394**	**0.404**
ETTm2	96	0.181	0.264	**0.178**	**0.262**	0.184	0.263	**0.183**	**0.262**	0.182	0.266	**0.178**	**0.262**
	192	0.248	0.307	**0.245**	**0.306**	0.250	0.304	**0.249**	**0.303**	0.247	0.308	**0.243**	**0.304**
	336	0.316	0.350	**0.313**	**0.348**	0.311	**0.342**	**0.310**	0.342	0.310	0.347	**0.304**	**0.343**
	720	0.425	0.413	**0.422**	**0.412**	**0.412**	**0.399**	0.412	0.399	0.410	0.404	**0.403**	**0.400**
	Avg.	0.293	0.334	**0.290**	**0.332**	**0.289**	**0.327**	0.289	0.327	0.287	0.331	**0.282**	**0.327**
Weather	96	0.203	0.253	**0.173**	**0.214**	0.174	0.210	**0.168**	**0.207**	0.178	0.216	**0.170**	**0.210**
	192	0.225	0.292	**0.219**	**0.257**	0.227	0.257	**0.220**	**0.253**	0.227	0.259	**0.218**	**0.254**
	336	0.303	0.326	**0.277**	**0.299**	0.283	0.298	**0.278**	**0.296**	0.282	0.299	**0.276**	**0.296**
	720	0.375	0.371	**0.365**	**0.356**	0.362	0.350	**0.359**	**0.348**	0.358	0.349	**0.351**	**0.347**
	Avg.	0.277	0.311	**0.259**	**0.282**	0.262	0.279	**0.256**	**0.276**	0.261	0.281	**0.254**	**0.277**
Solar-Energy	96	0.200	0.235	**0.197**	**0.234**	0.210	0.226	**0.203**	**0.220**	0.207	0.235	**0.199**	**0.226**
	192	**0.248**	**0.266**	0.251	0.269	0.233	0.251	**0.225**	**0.245**	0.242	0.266	**0.228**	**0.258**
	336	**0.300**	**0.298**	0.301	0.299	0.244	0.267	**0.241**	**0.264**	0.252	0.278	**0.240**	**0.270**
	720	0.378	0.338	**0.365**	**0.336**	**0.247**	**0.270**	0.247	0.273	0.249	0.279	**0.247**	**0.278**
	Avg.	0.282	**0.284**	**0.279**	0.285	0.234	0.254	**0.229**	**0.251**	0.238	0.265	**0.229**	**0.258**
ECL	96	**0.136**	**0.230**	0.136	0.230	0.143	0.233	**0.142**	**0.231**	**0.146**	0.240	0.148	**0.239**
	192	0.158	0.252	**0.157**	**0.250**	0.159	0.249	**0.156**	**0.246**	**0.163**	**0.255**	0.164	0.255
	336	0.180	0.277	**0.177**	**0.272**	0.172	0.264	**0.170**	**0.263**	**0.178**	**0.271**	0.180	0.271
	720	0.242	0.333	**0.232**	**0.321**	0.203	**0.293**	**0.202**	0.293	0.209	0.300	**0.208**	**0.297**
	Avg.	0.179	0.273	**0.176**	**0.268**	0.169	0.260	**0.168**	**0.258**	**0.174**	0.267	0.175	**0.266**
Traffic	96	0.387	0.259	**0.384**	**0.257**	0.392	0.259	**0.390**	**0.257**	0.394	0.266	**0.392**	**0.264**
	192	0.418	0.276	**0.415**	**0.275**	0.419	0.271	**0.415**	**0.268**	0.420	0.276	**0.415**	**0.274**
	336	0.448	**0.290**	**0.447**	0.299	0.435	0.279	**0.430**	**0.276**	0.436	0.284	**0.432**	**0.282**
	720	0.518	0.325	**0.496**	**0.323**	0.464	0.296	**0.461**	0.294	0.468	0.301	**0.465**	**0.300**
	Avg.	0.443	**0.288**	**0.436**	0.289	0.428	0.276	**0.424**	**0.274**	0.430	0.282	**0.426**	**0.280**
PEMS03	12	-	-	-	-	0.068	**0.171**	**0.067**	0.171	**0.069**	**0.174**	0.070	0.174
	24	-	-	-	-	**0.095**	0.204	0.095	**0.202**	0.098	0.208	**0.096**	**0.206**
	48	-	-	-	-	0.155	0.262	**0.151**	**0.257**	0.159	0.269	**0.158**	**0.264**
	96	-	-	-	-	0.232	0. 331	**0.219**	**0.318**	0.242	0.342	**0.230**	**0.327**
	Avg.	-	-	-	-	0.138	0.242	**0.133**	**0.237**	0.142	0.248	**0.139**	**0.243**
PEMS08	12	-	-	-	-	0.078	0.177	**0.076**	**0.173**	0.080	0. 181	**0.078**	**0.177**
	24	-	-	-	-	0.112	0.210	**0.107**	**0.204**	0.116	0.217	**0.111**	**0.210**
	48	-	-	-	-	0.185	0.267	**0.174**	**0.258**	0.196	0.281	**0.183**	**0.267**
	96	-	-	-	-	0.312	0.344	**0.288**	**0.327**	0.338	0.373	**0.297**	**0.339**
	Avg.	-	-	-	-	0.172	0.250	**0.161**	**0.241**	0.183	0.263	**0.167**	**0.248**

I Forecasting Accuracy Visualization

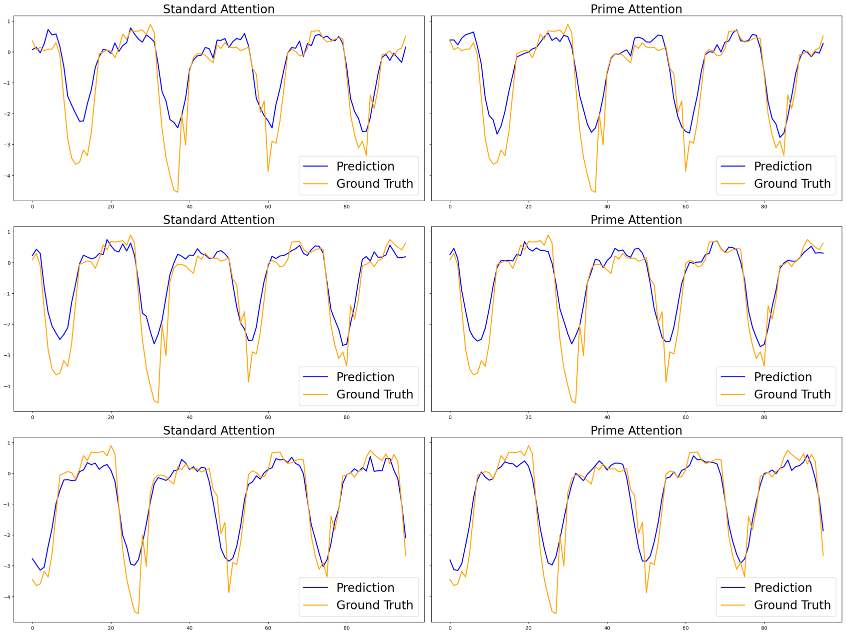

Figure 9: Forecasting visualization on ETTh1 dataset using predictions (in blue) made from standard attention (left) and prime attention (right) against ground-truth labels (in yellow). Each row represents a random batch.

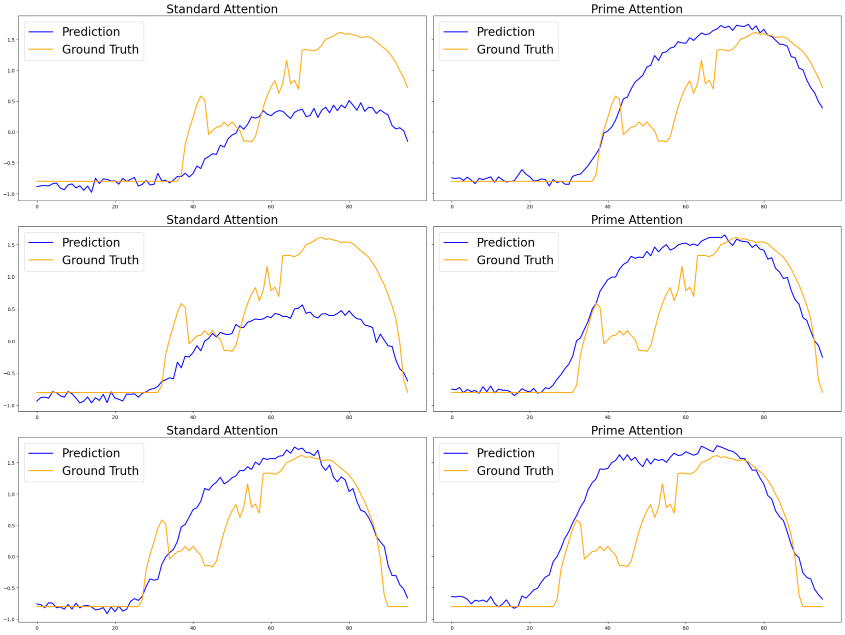

Figure 10: Forecasting visualization on Solar dataset using predictions (in blue) made from standard attention (left) and prime attention (right) against ground-truth labels (in yellow). Each row represents a random batch.